arXiv:1611.01629v4 [cs.SY] 12 Jan 2017

On the optimal feedforward torque control problem of anisotropic synchronous machines: Quadrics, quartics and analytical solutions

Hisham Eldeeb[‡], Christoph M. Hackl[‡,⋆], Lorenz Horlbeck[†] and Julian Kullick[‡]

Abstract

The optimal feedforward torque control problem is tackled and solved analytically for synchronous machines while stator resistance and cross-coupling inductance are explicitly considered. Analytical solutions for the direct and quadrature optimal reference currents are found for all major operation strategies such as Maximum Torque per Current (MTPC) (or often called as Maximum Torque per Ampere (MTPA)), Maximum Current (MC), Field Weakening (FW), Maximum Torque per Voltage (MTPV) and Maximum Torque per Flux (MTPF). Numerical methods (approximating the optimal solutions only) or simplifying assumptions (neglecting stator resistance and/or cross-coupling inductance) are *no longer* necessary. The presented results are based on one simple idea: all optimization problems (e.g. MTPC, MTPV or MTPF) with their respective constraints (e.g. current or voltage limit) and the computation of the intersection point(s) of voltage ellipse, current circle, or torque, MTPC, MTPV and MTPF hyperbolas are reformulated implicitly as *quadrics* (quadratic surfaces) which allow to solve the feedforward torque control problem by invoking the Lagrangian formalism and by finding the roots of a fourth-order polynomial analytically. The proposed solutions are applicable to any anisotropic (or isotropic) synchronous machine independent of the underlying current control strategy.

Keywords—Maximum Torque per Ampere (MTPA), Maximum Torque per Current (MTPC), Maximum Torque per Voltage (MTPV), Maximum Torque per Flux (MTPF), Maximum Current (MC), Field Weakening (FW), analytical solution, optimal feedforward torque control, anisotropy, synchronous machine, interior permanent-magnet synchronous machine, reluctance synchronous machine, permanent-magnet assisted or enhanced synchronous machine, quadrics, quartics, Lagrangian optimization

NOTATION

$\mathbb{N}, \mathbb{R}, \mathbb{C}$: natural, real, complex numbers. $\boldsymbol{x} := (x_1, \dots, x_n)^\top \in \mathbb{R}^n$: column vector, $n \in \mathbb{N}$ where "$^\top$" and ":=" mean "transposed" (interchanging rows and columns of a matrix or vector) and "is defined as", resp., $\boldsymbol{0}_n \in \mathbb{R}^n$: zero vector. $\boldsymbol{a}^\top \boldsymbol{b} := a_1 b_1 + \dots + a_n b_n$: scalar product of the vectors $\boldsymbol{a} := (a_1, \dots, a_n)^\top$ and $\boldsymbol{b} := (b_1, \dots, b_n)^\top$. $\|\boldsymbol{x}\| := \sqrt{\boldsymbol{x}^\top \boldsymbol{x}} = \sqrt{x_1^2 + \dots + x_n^2}$: Euclidean norm of $\boldsymbol{x}$. $\boldsymbol{A} \in \mathbb{R}^{n \times n}$: (square) matrix with n rows and columns. $\boldsymbol{A}^{-1}$: inverse of $\boldsymbol{A}$ (if exists). $\det(\boldsymbol{A})$: determinant of $\boldsymbol{A}$, $\operatorname{spec}(\boldsymbol{A})$: spectrum of $\boldsymbol{A}$ (the set of the eigenvalues of $\boldsymbol{A}$). $\boldsymbol{I}_n \in \mathbb{R}^{n \times n} := \operatorname{diag}(1, \dots, 1)$: identity matrix. $\boldsymbol{O}_{n \times p} \in \mathbb{R}^{n \times p}$: zero matrix, $n, p \in \mathbb{N}$. $\boldsymbol{T}_\mathrm{p}(\phi_\mathrm{k}) = \left[\begin{smallmatrix} \cos(\phi_\mathrm{k}) & -\sin(\phi_\mathrm{k}) \\ \sin(\phi_\mathrm{k}) & \cos(\phi_\mathrm{k}) \end{smallmatrix}\right]$: Park transformation matrix (with electrical angle ϕ_k) and $\boldsymbol{J} := \boldsymbol{T}_\mathrm{p}(\pi/2) = \left[\begin{smallmatrix} 0 & -1 \\ 1 & 0 \end{smallmatrix}\right]$: rotation matrix (counter-clock wise rotation by $\frac{\pi}{2}$; see e.g. [1], [2]). "s.t.": subject to (optimization with constraints). $\jmath$: imaginary unit with $\jmath^2 = \sqrt{-1}$, "$\stackrel{!}{=}$": must equal. $X \cap Y$: intersection of the sets X and Y (in this paper: X, $Y \subset \mathbb{R}^2$).

CONTENTS

I Introduction 2

II Problem formulation 3
- II-A Generic dynamical model of synchronous machines (SMs) . . . 3
- II-B Operation constraints . . . 4
- II-C Problem formulation . . . 4

III Mathematical preliminaries: Steady-state operation and implicit formulations 5
- III-A Steady-state operation . . . 5
- III-B Implicit formulation of machine torque and constraints as quadrics . . . 5
  - III-B1 Torque hyperbola (constant torque trajectory) . . . 6
  - III-B2 Voltage elliptical area (reformulation of the voltage constraint in (5)) . . . 6
  - III-B3 Current circular area (reformulation of the current constraint in (5)) . . . 8
  - III-B4 Flux norm . . . 8

[‡]H. Eldeeb, C.M. Hackl and J. Kullick are with the research group "Control of renewable energy systems" (CRES) at the Munich School of Engineering (MSE), Technische Universität München (TUM), Germany.

[†]L. Horlbeck is with the Institute of Automotive Technology (FTM), Technische Universität München (TUM), Germany.

[⋆]Authors are in alphabetical order and contributed equally to the paper. Corresponding author is C.M. Hackl (christoph.hackl@tum.de).

IV Operation strategies 8
IV-A Maximum-Torque-per-Current (MTPC) hyperbola (considering L_m) . . . 8
IV-B Maximum current (MC) . . . 9
IV-C Field weakening (FW) . . . 9
IV-D Maximum-Torque-per-Voltage (MTPV) hyperbola (considering R_s and L_m) . . . 9
IV-E Maximum-Torque-per-Flux (MTPF) hyperbola (considering L_m) . . . 10
IV-F Analytical solutions of the optimal reference current vector for MTPC, MC, FW, MTPV and MTPF . . . 11
IV-G Graphical illustration of the operation strategies MPTC, FW and MTPV . . . 11

Appendix 12
A Formulation of the optimization problem with equality constraints . . . 13
A1 Necessary condition for a maximum . . . 13
A2 Sufficient condition for a maximum . . . 14
A3 Analytical computation of the roots of a quartic polynomial . . . 15
A4 Analytical computation of the roots of a cubic polynomial . . . 16
B Computation of the quadrics (implicit expressions) for MTPC, MTPV and MTPF . . . 16
C Explicit expressions for current circle, voltage ellipse, and torque, MTPC, MTPV and MTPF hyperbolas 17
D Computation of the intersection points of two arbitrary quadrics . . . 17

References 18

I. Introduction

The efficient use of electrical energy becomes more and more significant; in particular for electrical machines. Electrical machines consume more than half of the globally generated electricity [3]. Hence, advances in research on the control and modeling of electrical drives (machine+inverter) have been made; in particular for synchronous machines (SMs) with non-negligible anisotropy such as *interior permanent-magnet (PM) synchronous motors (IPMSMs)*, *reluctance synchronous machines (RSMs)*, *PM-assisted RSMs (PMA-RSMs)* or *PM-enhanced RSMs (PME-RSMs)* [4]–[6]. The two approaches for enhancing the efficiency of SMs are (a) improving the stator or rotor design of the electrical machine [4], [5], [7] or (b) extracting the highest possible efficiency by implementing an optimal feedforward torque control strategy (which is the topic under study in this paper).

Optimization of torque production while minimizing copper losses at *steady state* can be classified into two categories (i) "*search control*" (SC) and (ii) "*loss model control*" (LMC). The SC approach is considered as a *perturb and observe* adaptive strategy which continuously approximates the minimizing reference currents online for any given reference torque. The SC method does not require precise knowledge of the machine parameters [8]. Nevertheless, stability of such a strategy is not always guaranteed [9]. On the other hand, LMC–*adopted in this paper*–is based on the development of a mathematical model, that describes the electromechanical conversion and electrical losses of the machine during operation. Clearly, LMC strictly depends on the machine parameters which are sometimes provided by the manufacturer or can be obtained through experiments [10], [11]. Depending on the current and voltage constraints, and the actual angular velocity and the demanded reference torque of the electrical drive system, *four* optimal feedforward torque control strategies can be defined: (a) *Maximum Torque per Current (MTPC)* (which, in literature, is also known as *Maximum Torque per Ampere (MTPA)*), (b) *Maximum Current (MC)*, (c) *Field Weakening (FW)* and (d) *Maximum Torque per Voltage (MPTV)* or *Maximum Torque per Flux (MTPF)*.

The optimal feedforward torque control problem has been investigated in numerous publications, see e.g. [12]–[25] for MTPC, [7], [16], [17], [25]–[27] for FW, and [16], [27]–[30] for MTPV to name a few. Note that the MPTF operation strategy, which minimizes the stator iron losses at high speeds [15], [31], is a special (simplified) case of the MTPV operation strategy (shown later in this paper). The online computation of the optimal reference currents for the different operation strategies (such as MTPC, MC, FW, MTPV or MTPF) is usually done *numerically* or *analytically but with simplifying assumptions* on the machine model (e.g. neglecting stator resistance and/or cross-coupling inductance) or the physical constraints (e.g. voltage ellipse). Moreover, numerical solutions in general come at the expense of tightening the programmed tolerances which may decrease the speed of the control algorithm and increase the computational load on the real-time system. Analytical solutions are more attractive, since they are easier to implement, more accurate and faster to compute. However, to the best knowledge of the authors, analytical solutions *including* stator resistance and mutual inductance for MTPC, MC, FW, MTPV and MTPF of anisotropic SMs are scarcely investigated or not available at all. For example, in [15, Sec. IV], [28, Sec. 2.2.3], and [31, Sec. II-B], it was stated that acquiring a general analytical solution of the optimal currents for MTPV and MTPF while considering non-negligible stator resistance and magnetic cross-coupling is or seems *not possible* and would introduce a high degree of complexity.

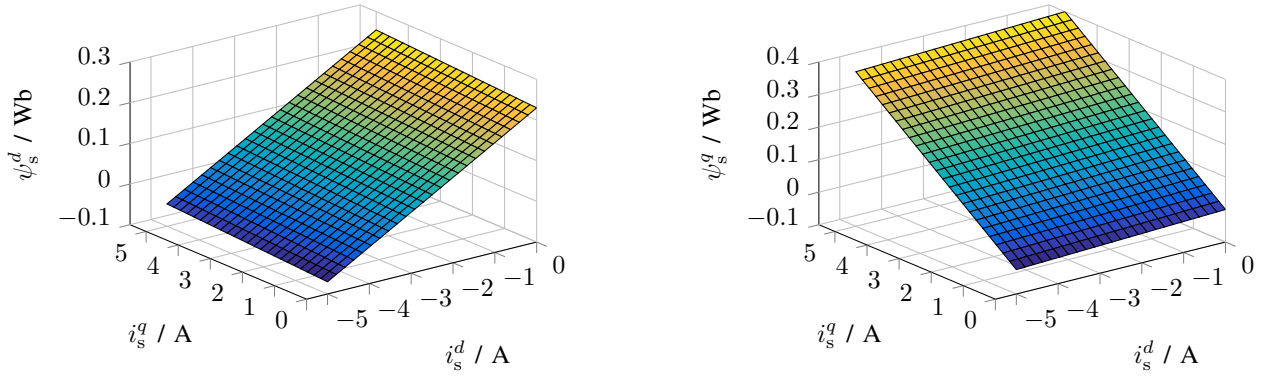

(a) *d-component* ψ_s^d *of the stator flux linkage.*

(b) *q-component* ψ_s^q *of the stator flux linkage.*

Figure 1: *Flux linkage map* (2) *of an exemplary SM with parameters as in* (36)*: Due to the non-zero mutual inductance, both flux linkage maps are slightly tilted (the map is only shown for the second quadrant, i.e.* $i_\mathrm{s}^d \leq 0$ *and* $i_\mathrm{s}^q \geq 0$*).*

Motivated by the aforementioned challenges and remaining open questions (e.g. how to consider stator resistance and cross-coupling in the whole feedforward torque control problem), the following research work has been conducted. The main contributions of this paper are:

(i) The derivation of a *unified theory for optimal feedforward torque control for anisotropic (and isotropic) SMs* which allows to compute the optimal reference currents *analytically* for *all* operation strategies (such as MTPC, MC, FW, MTPV and MTPF) incorporating *stator resistance* and *cross-coupling (mutual) inductance*. Moreover, the proposed analytical solutions offer (a) guaranteed convergence to the optimal reference currents (compared to numerical methods), (b) easy and straight-forward implementation, and (c) rapid execution and low computational burden making the proposed analytical algorithms very suitable even for modest (hence cheap) processor boards.

(ii) The unified theory is established by (a) the use of *Lagrangian multipliers* and (b) an *implicit* problem formulation as *quadrics* (i.e. all trajectories of constraints and operation strategies in the (d,q)-plane–such as e.g. current circle, voltage ellipse and torque hyperbola–are reformulated implicitly as quadric surfaces).

(iii) It is shown that *only* for very high speeds or very small stator resistances, the MTPF solution is an acceptable approximation of the MTPV solution. In general, an MTPV algorithm incorporating stator resistance and mutual inductance yields higher efficiencies and should be preferred and implemented.

(iv) The negative effects of neglecting stator resistance and mutual inductance or both on the optimality of all operation strategies are illustrated, which show that neglecting these two parameters during optimization will lead to significant deviations between optimal and approximated reference currents.

The remainder of the paper is organized as follows: Section II re-visits the dynamic model of anisotropic synchronous machines, its operation constraints (such as current and voltage constraint) and the problem formulation of optimal feedforward torque control. Section III deals with mathematical preliminaries at steady state and the implicit reformulations (as quadrics) of the optimization problems and machine constraints. This paves the way for Section IV, where the *analytical* solutions for MTPC, MC, FW, MTPV and MTPF are presented. To improve readability, the thorough mathematical derivations of the unified theory are collected and summarized in the Appendices A-D.

II. Problem formulation

A. Generic dynamical model of synchronous machines (SMs)

The model of an anisotropic (a) permanent-magnet synchronous machine (PMSM), (b) permanent-magnet assisted or excited reluctance synchronous machine (PMA-RSM or PME-RSM, resp. [6], [23]) or (c) reluctance synchronous machine (RSM [6], [32], [33]) in the (d,q)-reference frame[1] is given by

$$\left.\begin{aligned}
&\overbrace{\begin{pmatrix} u_\mathrm{s}^d(t) \\ u_\mathrm{s}^q(t) \end{pmatrix}}^{=:\boldsymbol{u}_\mathrm{s}^k(t)} = R_\mathrm{s} \overbrace{\begin{pmatrix} i_\mathrm{s}^d(t) \\ i_\mathrm{s}^q(t) \end{pmatrix}}^{=:\boldsymbol{i}_\mathrm{s}^k(t)} + \omega_\mathrm{k}(t) \overbrace{\begin{bmatrix} 0 & -1 \\ 1 & 0 \end{bmatrix}}^{=:\boldsymbol{J}} \overbrace{\begin{pmatrix} \psi_\mathrm{s}^d\big(\boldsymbol{i}_\mathrm{s}^k(t)\big) \\ \psi_\mathrm{s}^q\big(\boldsymbol{i}_\mathrm{s}^k(t)\big) \end{pmatrix}}^{=:\boldsymbol{\psi}_\mathrm{s}^k\left(\boldsymbol{i}_\mathrm{s}^k(t)\right)} + \tfrac{\mathrm{d}}{\mathrm{d}t}\boldsymbol{\psi}_\mathrm{s}^k(\boldsymbol{i}_\mathrm{s}^k(t)), \qquad \boldsymbol{\psi}_\mathrm{s}^k(\boldsymbol{i}_\mathrm{s}^k(0)) = \boldsymbol{\psi}_\mathrm{s}^{k,0} \in \mathbb{R}^2 \\
&\tfrac{\mathrm{d}}{\mathrm{d}t}\omega_\mathrm{k}(t) = \frac{n_\mathrm{p}}{\Theta}\Big(m_\mathrm{m}(\boldsymbol{i}_\mathrm{s}^k(t)) - m_\mathrm{l}(t)\Big), \qquad \omega_\mathrm{k}(0) = n_\mathrm{p}\omega_\mathrm{m}^0 \in \mathbb{R} \\
&\tfrac{\mathrm{d}}{\mathrm{d}t}\phi_\mathrm{k}(t) = \omega_\mathrm{k}(t), \qquad \phi_\mathrm{k}(0) = n_\mathrm{p}\phi_\mathrm{m}^0 \in \mathbb{R}.
\end{aligned}\right\} \tag{1}$$

[1] I.e., the synchronously rotating $k=(d,q)$-coordinate system with orthogonal axes d and q after Clarke and Park transformation [1], [2].

with initial values $\boldsymbol{\psi}_{\mathrm{s}}^{k,0}$, ω_{m}^0 and ϕ_{m}^0. The following assumption is imposed on the flux linkage:

Assumption II.1. *For a (locally)* constant *inductance matrix $\boldsymbol{L}_{\mathrm{s}}^k \in \mathbb{R}^{2\times 2}$ (e.g. obtained by a linearization of* (1) *at the actual operating point), the (local approximation of the) flux linkage can be expressed as follows*

$$\boldsymbol{\psi}_{\mathrm{s}}^k\big(\boldsymbol{i}_{\mathrm{s}}^k(t)\big) = \underbrace{\begin{bmatrix} L_{\mathrm{s}}^d & L_{\mathrm{m}} \\ L_{\mathrm{m}} & L_{\mathrm{s}}^q \end{bmatrix}}_{=:\boldsymbol{L}_{\mathrm{s}}^k \in \mathbb{R}^{2\times 2}} \boldsymbol{i}_{\mathrm{s}}^k(t) + \underbrace{\begin{pmatrix} \psi_{\mathrm{pm}}^d \\ \psi_{\mathrm{pm}}^q \end{pmatrix}}_{=:\boldsymbol{\psi}_{\mathrm{pm}}^k} \quad \textit{where} \quad \boldsymbol{\psi}_{\mathrm{pm}}^k = \begin{cases} (\psi_{\mathrm{pm}}, 0)^\top, & \textit{for PMSM and PME-RSM [6]} \\ (0, -\psi_{\mathrm{pm}})^\top, & \textit{for PMA-RSM [6], [23]} \\ (0,0)^\top, & \textit{for RSM [6], [32], [33].} \end{cases} \tag{2}$$

Then, the machine torque can be computed as follows

$$m_{\mathrm{m}}\big(\boldsymbol{i}_{\mathrm{s}}^k(t)\big) = \tfrac{3}{2} n_{\mathrm{p}}\, \boldsymbol{i}_{\mathrm{s}}^k(t)^\top \boldsymbol{J} \boldsymbol{\psi}_{\mathrm{s}}^k\big(\boldsymbol{i}_{\mathrm{s}}^k(t)\big) \overset{(2)}{=} \tfrac{3}{2} n_{\mathrm{p}} \left[\boldsymbol{i}_{\mathrm{s}}^k(t)^\top \boldsymbol{J} \boldsymbol{L}_{\mathrm{s}}^k \boldsymbol{i}_{\mathrm{s}}^k(t) + \boldsymbol{i}_{\mathrm{s}}^k(t)^\top \boldsymbol{J} \boldsymbol{\psi}_{\mathrm{pm}}^k\right] \tag{3}$$

$$= \tfrac{3}{2}\, n_{\mathrm{p}} \Big[\psi_{\mathrm{pm}}^d i_{\mathrm{s}}^q(t) - \psi_{\mathrm{pm}}^q i_{\mathrm{s}}^d(t) + \big(L_{\mathrm{s}}^d - L_{\mathrm{s}}^q\big) i_{\mathrm{s}}^d(t) i_{\mathrm{s}}^q(t) + L_{\mathrm{m}}\big(i_{\mathrm{s}}^q(t)^2 - i_{\mathrm{s}}^d(t)^2\big)\Big] \tag{4}$$

$$\overset{(2)}{=} \begin{cases} \tfrac{3}{2}\, n_{\mathrm{p}} \Big[\psi_{\mathrm{pm}} i_{\mathrm{s}}^q(t) + \big(L_{\mathrm{s}}^d - L_{\mathrm{s}}^q\big) i_{\mathrm{s}}^d(t) i_{\mathrm{s}}^q(t) + L_{\mathrm{m}}\big(i_{\mathrm{s}}^q(t)^2 - i_{\mathrm{s}}^d(t)^2\big)\Big], & \text{for PMSM or PME-RSM} \\ \tfrac{3}{2}\, n_{\mathrm{p}} \Big[\psi_{\mathrm{pm}} i_{\mathrm{s}}^d(t) + \big(L_{\mathrm{s}}^d - L_{\mathrm{s}}^q\big) i_{\mathrm{s}}^d(t) i_{\mathrm{s}}^q(t) + L_{\mathrm{m}}\big(i_{\mathrm{s}}^q(t)^2 - i_{\mathrm{s}}^d(t)^2\big)\Big], & \text{for PMA-RSM,} \\ \tfrac{3}{2}\, n_{\mathrm{p}} \Big[\big(L_{\mathrm{s}}^d - L_{\mathrm{s}}^q\big) i_{\mathrm{s}}^d(t) i_{\mathrm{s}}^q(t) + L_{\mathrm{m}}\big(i_{\mathrm{s}}^q(t)^2 - i_{\mathrm{s}}^d(t)^2\big)\Big], & \text{for RSM.} \end{cases}$$

In (1), (2) and (3) or (4), R_{s} (in Ω) is the stator resistance, $\boldsymbol{u}_{\mathrm{s}}^k := (u_{\mathrm{s}}^d, u_{\mathrm{s}}^q)^\top$ (in V), $\boldsymbol{i}_{\mathrm{s}}^k := (i_{\mathrm{s}}^d,\, i_{\mathrm{s}}^q)^\top$ (in A) and $\boldsymbol{\psi}_{\mathrm{s}}^k := (\psi_{\mathrm{s}}^d,\, \psi_{\mathrm{s}}^q)^\top$ (in Wb) are stator voltage (e.g. applied by a voltage source inverter), current and flux linkage vectors in the (d,q)-reference frame, respectively. Note that $\omega_{\mathrm{k}} = n_{\mathrm{p}}\, \omega_{\mathrm{m}}$ (in $\mathrm{rad/s}$) and $\phi_{\mathrm{k}} = n_{\mathrm{p}} \phi_{\mathrm{m}}$ are *electrical* angular frequency and angle, whereas ω_{m} and ϕ_{m} are *mechanical* angular frequency and angle of the rotor (with initial values ω_{m}^0 and ϕ_{m}^0), respectively. n_{p} is the pole pair number of the machine and Θ (in $\mathrm{kg\,m^2}$) is the (rotor's) inertia. m_{m} is the electro-magnetic machine torque[2] and m_{l} (in Nm) is a (bounded) load torque. The flux linkage $\boldsymbol{\psi}_{\mathrm{s}}^k$ depends on the *symmetric*, *positive-definite* inductance matrix $\boldsymbol{L}_{\mathrm{s}}^k = (\boldsymbol{L}_{\mathrm{s}}^k)^\top > 0$ [32] with stator inductances $L_{\mathrm{s}}^q > 0$, $L_{\mathrm{s}}^d > 0$ (both in H) and cross-coupling (mutual) inductance[3] $L_{\mathrm{m}} \in \mathbb{R}$ (in H) and $L_{\mathrm{s}}^d L_{\mathrm{s}}^q - L_{\mathrm{m}}^2 > 0$, the stator currents $\boldsymbol{i}_{\mathrm{s}}^k$ and the permanent-magnet flux linkage $\boldsymbol{\psi}_{\mathrm{pm}}^k = (\psi_{\mathrm{pm}}^d,\, \psi_{\mathrm{pm}}^q)^\top$. Fig. 1 illustrates the flux linkage (2) of an anisotropic IPMSM for some exemplified values of L_{s}^q, L_{s}^d, L_{m} and ψ_{pm}.

Remark II.2 (Affine flux linkage)**.** *Note that Assumption II.1 implies a (locally) constant inductance matrix; this is in line with most recent publications (even from 2016) which also deal with constant inductances only (see e.g. [12], [17], [24], [27], [35]–[37] for PMSMs or [28], [38] for RSMs). This simplification will* not *be true in the most general case when the flux linkage is a nonlinear function of the currents [11], [33]. Nevertheless, in the humble opinion of the authors, the presented results are of quite some relevance and have not been discussed in this general framework before: The results of this paper can be considered as a generalization of the results for IPMSM in [16] by including resistance R_{s} and mutual inductance L_{m} into the generic optimization formulation. The simplifying assumptions which neglect these physical parameters are overcome. The consideration of nonlinear flux linkages is ongoing research.*

B. Operation constraints

Due to safety and physical reasons [34, Cha. 16], stator currents and voltages should never exceed their respective maximal amplitudes $\hat{\imath}_{\max} > 0$ (in A) and $\hat{u}_{\max} > 0$ (in V). Hence, the following must be ensured by the control system for all time

$$\forall t \geq 0\,\mathrm{s}\colon \qquad \|\boldsymbol{i}_{\mathrm{s}}^k(t)\|^2 = i_{\mathrm{s}}^d(t)^2 + i_{\mathrm{s}}^q(t)^2 \leq \hat{\imath}_{\max}(t)^2 \qquad \text{and} \qquad \|\boldsymbol{u}_{\mathrm{s}}^k(t)\|^2 = u_{\mathrm{s}}^d(t)^2 + u_{\mathrm{s}}^q(t)^2 \leq \hat{u}_{\max}(t)^2. \tag{5}$$

Note that maximally admissible current $\hat{\imath}_{\max}$ and voltage $\hat{u}_{\max}$ might change over time: (a) the current limit is usually equal to the nominal/rated current of the machine but can also exceed this nominal value for a short period in time and (b) the maximally applicable voltage will change with the DC-link voltage of the inverter. In the remainder of this paper, the time-dependency will not be highlighted explicitly and the argument (t) will be dropped.

C. Problem formulation

For a given reference torque $m_{\mathrm{m,ref}}$ (in $\mathrm{N\,m}$) (and given current and voltage limits), the general control objective is to find analytical solutions of the optimal reference currents for all operation modes (such as e.g. MTPC, MTPF and MTPV). From a mathematical point of view, the following optimization problem

$$\max_{\boldsymbol{i}_{\mathrm{s}}^k} \; -f(\boldsymbol{i}_{\mathrm{s}}^k) \;\; \text{s.t.} \;\; \|\boldsymbol{u}_{\mathrm{s}}^k\| \leq \hat{u}_{\max},\; \|\boldsymbol{i}_{\mathrm{s}}^k\| \leq \hat{\imath}_{\max},\; |m_{\mathrm{m}}(\boldsymbol{i}_{\mathrm{s}}^k)| \leq |m_{\mathrm{m,ref}}| \;\; \text{and} \;\; \operatorname{sign}(m_{\mathrm{m,ref}}) = \operatorname{sign}(m_{\mathrm{m}}(\boldsymbol{i}_{\mathrm{s}}^k)) \tag{6}$$

[2]The factor $3/2$ is due to an amplitude-correct Clarke transformation [34, Sec. 16.7].

[3]Note that the mutual inductance L_{m} changes its sign with the negative product of the currents, i.e. $\operatorname{sign}(L_{\mathrm{m}}) = -\operatorname{sign}(i_{\mathrm{s}}^d \cdot i_{\mathrm{s}}^q)$ [33, Fig. 2].

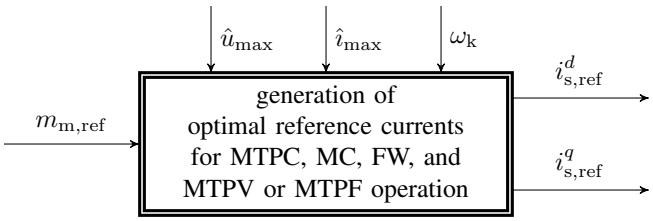

Figure 2: *Optimal reference current generation for a given reference torque $m_{\mathrm{m,ref}}$: The computed, optimal reference currents $i^d_{\mathrm{s,ref}}$ and $i^q_{\mathrm{s,ref}}$ depend also on maximal current $\hat{\imath}_{\max}$, maximal voltage $\hat{u}_{\max}$ and (actual) electrical angular frequency $\omega_{\mathrm{k}} = n_{\mathrm{p}}\omega_{\mathrm{m}}$.*

with three inequality constraints and one equality constraint must be solved online, where obviously the sign of reference and machine torque should coincide. The function $f(\boldsymbol{i}^k_{\mathrm{s}})$ depends on the operation strategy (e.g. $f(\boldsymbol{i}^k_{\mathrm{s}}) = \|\boldsymbol{i}^k_{\mathrm{s}}\|^2$ for MTPC; for more details, see Sec. IV), The most favorable outcome is an analytical solution which gives explicitly the reference current vector

$$\boxed{\boldsymbol{i}^k_{\mathrm{s,ref}}(m_{\mathrm{m,ref}}, \hat{u}_{\max}, \hat{\imath}_{\max}, \omega_{\mathrm{k}}) = \begin{pmatrix} i^d_{\mathrm{s,ref}}(m_{\mathrm{m,ref}}, \hat{u}_{\max}, \hat{\imath}_{\max}, \omega_{\mathrm{k}}) \\ i^q_{\mathrm{s,ref}}(m_{\mathrm{m,ref}}, \hat{u}_{\max}, \hat{\imath}_{\max}, \omega_{\mathrm{k}}) \end{pmatrix} := \arg\max_{\boldsymbol{i}^k_{\mathrm{s}}} m_{\mathrm{m}}(\boldsymbol{i}^k_{\mathrm{s}})} \tag{7}$$

as function (see Fig. 2) of reference torque $m_{\mathrm{m,ref}}$ (coming from an outer control loop; e.g. the speed control loop), voltage limit $\hat{u}_{\max}$, current limit $\hat{\imath}_{\max}$ and electrical angular velocity $\omega_{\mathrm{k}} = n_{\mathrm{p}}\omega_{\mathrm{m}}$. The computed reference current vector $\boldsymbol{i}^k_{\mathrm{s,ref}}$ can then directly be handed over to any underlying current control loop(s).

Remark II.3 (Feasible reference torques and non-convexity of the machine torque)**.** *Note that, due to the voltage limit (during high-speed operation) or due to the current limit, the range of admissible reference torques is restricted. Hence, not all reference torques $m_{\mathrm{m,ref}}$ are feasible during all operation modes, therefore the additional inequality constraint in* (6) *must be added. If the requested reference torque is feasible, the inequality constraint becomes the equality constraint $|m_{\mathrm{m}}(\boldsymbol{i}^k_{\mathrm{s}})| = |m_{\mathrm{m,ref}}|$ (or simply, $m_{\mathrm{m}}(\boldsymbol{i}^k_{\mathrm{s}}) = m_{\mathrm{m,ref}}$). Important to note that the machine torque $m_{\mathrm{m}}(\boldsymbol{i}^k_{\mathrm{s}}) \propto (\boldsymbol{i}^k_{\mathrm{s}})^\top \boldsymbol{J}\boldsymbol{L}^k_{\mathrm{s}}\boldsymbol{i}^k_{\mathrm{s}}$ is* not *convex, since $\boldsymbol{J}\boldsymbol{L}^k_{\mathrm{s}} = \begin{bmatrix} -L_{\mathrm{m}} & -L^q_{\mathrm{s}} \\ L^d_{\mathrm{s}} & L_{\mathrm{m}} \end{bmatrix}$ is non-symmetric and indefinite with eigenvalues $\pm\sqrt{L^2_{\mathrm{m}} - L^d_{\mathrm{s}}L^q_{\mathrm{s}}}$. Hence, maximizing the machine torque is not a viable approach. To account for that, the general optimization problem* (6) *will be divided into several sub-problems leading to the optimal operation strategies MTPC, MC, FW, MTPV or MTPF.*

III. Mathematical preliminaries: Steady-state operation and implicit formulations

A. Steady-state operation

In the remainder of this paper, only steady-state operation will be considered; which implies that $\frac{\mathrm{d}}{\mathrm{d}t}\boldsymbol{\psi}^k_{\mathrm{s}}(\boldsymbol{i}^k_{\mathrm{s}}) = \frac{\mathrm{d}}{\mathrm{d}t}\boldsymbol{i}^k_{\mathrm{s}} = \boldsymbol{0}_2$. Inserting (2) into (1) and neglecting the time derivative of the current, i.e. $\frac{\mathrm{d}}{\mathrm{d}t}\boldsymbol{i}^k_{\mathrm{s}} = \boldsymbol{0}_2$, the steady-state stator circuit model of a SM in matrix/vector notation is obtained as follows

$$\boldsymbol{u}^k_{\mathrm{s}} = R_{\mathrm{s}}\boldsymbol{i}^k_{\mathrm{s}} + \omega_{\mathrm{k}}\boldsymbol{J}\boldsymbol{L}^k_{\mathrm{s}}\boldsymbol{i}^k_{\mathrm{s}} + \omega_{\mathrm{k}}\boldsymbol{J}\boldsymbol{\psi}^k_{\mathrm{pm}} \tag{8}$$

where $\boldsymbol{J}$, and $\boldsymbol{L}^k_{\mathrm{s}}$ and $\boldsymbol{\psi}^k_{\mathrm{pm}}$ are as in (1) and (2), respectively.

B. Implicit formulation of machine torque and constraints as quadrics

The steady-state SM model (8) will be the basis for all upcoming derivations. The trick to obtain and derive a unified theory for the optimal torque control problem under current and voltage constraints is the re-formulation of the general optimization problem (6) *implicitly by quadrics (or quadric surfaces)* which will allow to invoke the Lagrangian formalism to derive an analytical solution for all different operation modes (such as MTPC, MTPV, FW, etc.). In the upcoming sections, the implicit forms of torque hyperbola, voltage ellipse (elliptical area), current circle (circular area) and flux norm are presented. The explicit forms are also given (as link to the existing literature) if their expressions are not too long. Stator resistance $R_{\mathrm{s}} \neq 0$ and mutual inductance $L_{\mathrm{m}} \neq 0$ will *not* be neglected to present the most general result achievable within the framework of affine flux linkages as in (2).

1) Torque hyperbola (constant torque trajectory): To derive the implicit form as quadric of the torque hyperbola, the following symmetric matrix, vector and constant are defined:

$$\left.\begin{aligned} \boldsymbol{T} &:= \tfrac{3}{4} n_{\mathrm{p}} \big(\boldsymbol{J} \boldsymbol{L}_{\mathrm{s}}^k + \boldsymbol{L}_{\mathrm{s}}^k \boldsymbol{J}^\top \big) = \tfrac{3}{2} n_{\mathrm{p}} \begin{bmatrix} -L_{\mathrm{m}} & \frac{L_{\mathrm{s}}^d - L_{\mathrm{s}}^q}{2} \\ \frac{L_{\mathrm{s}}^d - L_{\mathrm{s}}^q}{2} & L_{\mathrm{m}} \end{bmatrix} = \boldsymbol{T}^\top, \\ \boldsymbol{t} &:= \tfrac{3}{4} n_{\mathrm{p}} \boldsymbol{J} \boldsymbol{\psi}_{\mathrm{pm}}^k = \tfrac{3}{2} n_{\mathrm{p}} \begin{pmatrix} -\frac{\psi_{\mathrm{pm}}^q}{2} \\ \frac{\psi_{\mathrm{pm}}^d}{2} \end{pmatrix} \overset{(2)}{=} \begin{cases} \frac{3}{2} n_{\mathrm{p}} \left(0, \quad \frac{\psi_{\mathrm{pm}}}{2} \right)^\top, & \text{for PMSM and PME-RSM} \\ \frac{3}{2} n_{\mathrm{p}} \left(\frac{\psi_{\mathrm{pm}}}{2}, \quad 0 \right)^\top, & \text{for PMA-RSM} \\ (0,\, 0)^\top, & \text{for RSM,} \end{cases} \\ \tau(m_{\mathrm{m,ref}}) &:= -m_{\mathrm{m,ref}}. \end{aligned}\right\} \tag{9}$$

Moreover, note that $(\boldsymbol{i}_{\mathrm{s}}^k)^\top \boldsymbol{J} \boldsymbol{L}_{\mathrm{s}}^k \boldsymbol{i}_{\mathrm{s}}^k = (\boldsymbol{i}_{\mathrm{s}}^k)^\top \boldsymbol{L}_{\mathrm{s}}^k \boldsymbol{J}^\top \boldsymbol{i}_{\mathrm{s}}^k$, hence

$$\tfrac{3}{4} n_{\mathrm{p}} (\boldsymbol{i}_{\mathrm{s}}^k)^\top (\boldsymbol{J} \boldsymbol{L}_{\mathrm{s}}^k + \boldsymbol{L}_{\mathrm{s}}^k \boldsymbol{J}^\top) \boldsymbol{i}_{\mathrm{s}}^k = (\boldsymbol{i}_{\mathrm{s}}^k)^\top \boldsymbol{T} \boldsymbol{i}_{\mathrm{s}}^k. \tag{10}$$

Now, by combining (9) and (10) with (3), the machine torque can be written as quadric as follows

$$m_{\mathrm{m}}(\boldsymbol{i}_{\mathrm{s}}^k) = (\boldsymbol{i}_{\mathrm{s}}^k)^\top \boldsymbol{T} \boldsymbol{i}_{\mathrm{s}}^k + 2 \boldsymbol{t}^\top \boldsymbol{i}_{\mathrm{s}}^k. \tag{11}$$

For machine torque $m_{\mathrm{m}}(\boldsymbol{i}_{\mathrm{s}}^k)$ as in (11) and *constant* reference torque $m_{\mathrm{m,ref}}$, the machine torque trajectory can be expressed implicitly as *torque hyperbola* by invoking (9) as follows

$$\boxed{\mathbb{T}(m_{\mathrm{m,ref}}) := \left\{ \, \boldsymbol{i}_{\mathrm{s}}^k \in \mathbb{R}^2 \;\middle|\; (\boldsymbol{i}_{\mathrm{s}}^k)^\top \boldsymbol{T} \boldsymbol{i}_{\mathrm{s}}^k + 2 \boldsymbol{t}^\top \boldsymbol{i}_{\mathrm{s}}^k + \tau(m_{\mathrm{m,ref}}) = 0 \, \right\}.} \tag{12}$$

An exemplary torque hyperbola is plotted in Fig. 3 (see —— line).

Remark III.1 (Explicit expression for the torque hyperbola)**.** *For e.g.* $i_{\mathrm{s}}^d \leq 0$ *and* $m_{\mathrm{m,ref}} > 0$*, the torque hyperbola can be expressed explicitly (by solving* (4) *for* i_{s}^q*):*

$$\mathbb{T}(i_{\mathrm{s}}^d, m_{\mathrm{m,ref}}) = \begin{cases} \dfrac{1}{3} \dfrac{3 \psi_{\mathrm{pm}}^q n_{\mathrm{p}} i_{\mathrm{s}}^d + 2\, m_{\mathrm{m,ref}}}{n_{\mathrm{p}} \big[\psi_{\mathrm{pm}}^d + (L_{\mathrm{s}}^d - L_{\mathrm{s}}^q)\, i_{\mathrm{s}}^d \big]}, & L_{\mathrm{m}} = 0 \\ -\dfrac{(L_{\mathrm{s}}^d - L_{\mathrm{s}}^q) i_{\mathrm{s}}^d + \psi_{\mathrm{pm}}^d}{2 L_{\mathrm{m}}} + & \\ + \dfrac{\sqrt{[(L_{\mathrm{s}}^d - L_{\mathrm{s}}^q)^2 + 4 L_{\mathrm{m}}^2]\, (i_{\mathrm{s}}^d)^2 + 2 \psi_{\mathrm{pm}}^d (L_{\mathrm{s}}^d - L_{\mathrm{s}}^q)\, i_{\mathrm{s}}^d + 4\, L_{\mathrm{m}} (i_{\mathrm{s}}^d \psi_{\mathrm{pm}}^q + \frac{2 m_{\mathrm{m,ref}}}{3p}) + (\psi_{\mathrm{pm}}^d)^2}}{2\, L_{\mathrm{m}}} & L_{\mathrm{m}} \neq 0, \end{cases} \tag{13}$$

which holds for all $i_{\mathrm{s}}^d \neq \psi_{\mathrm{pm}} / (L_{\mathrm{s}}^d - L_{\mathrm{s}}^q)$*. Note that the explicit expression* (13) *relies on a case study for the mutual inductance (and the signs of current* i_{s}^d *and reference torque* $m_{\mathrm{m,ref}}$*). The implicit form* (12) *holds in general and can easily be plotted (e.g. in Matlab using the command* `ezplot`*).*

2) Voltage elliptical area (reformulation of the voltage constraint in (5)*):* Recall that $\boldsymbol{J}^\top \boldsymbol{J} = \boldsymbol{I}_2$, $\alpha^\top = \alpha \in \mathbb{R}$ (the transpose of a scalar is the scalar itself), $(\boldsymbol{M}\boldsymbol{N})^\top = \boldsymbol{N}^\top \boldsymbol{M}^\top$ (for matrices of appropriate size) and $(\boldsymbol{L}_{\mathrm{s}}^k)^\top = \boldsymbol{L}_{\mathrm{s}}^k > 0$. With that in mind, inserting (8) into (5) and squaring the result yield

$$\begin{aligned} \hat{u}_{\max}^2 &\geq \|\boldsymbol{u}_{\mathrm{s}}^k\|^2 = (\boldsymbol{u}_{\mathrm{s}}^k)^\top \boldsymbol{u}_{\mathrm{s}}^k = (u_{\mathrm{s}}^d)^2 + (u_{\mathrm{s}}^q)^2 \\ &\overset{(8)}{\geq} R_{\mathrm{s}}^2 (\boldsymbol{i}_{\mathrm{s}}^k)^\top \boldsymbol{I}_2 \boldsymbol{i}_{\mathrm{s}}^k + R_{\mathrm{s}} \omega_{\mathrm{k}} (\boldsymbol{i}_{\mathrm{s}}^k)^\top \boldsymbol{J} \boldsymbol{L}_{\mathrm{s}}^k \boldsymbol{i}_{\mathrm{s}}^k + R_{\mathrm{s}} \omega_{\mathrm{k}} (\boldsymbol{i}_{\mathrm{s}}^k)^\top \boldsymbol{J} \boldsymbol{\psi}_{\mathrm{pm}}^k + \omega_{\mathrm{k}}^2 (\boldsymbol{i}_{\mathrm{s}}^k)^\top \underbrace{(\boldsymbol{L}_{\mathrm{s}}^k)^\top \boldsymbol{J}^\top \boldsymbol{J} \boldsymbol{L}_{\mathrm{s}}^k}_{=(\boldsymbol{L}_{\mathrm{s}}^k)^2} \boldsymbol{i}_{\mathrm{s}}^k + R_{\mathrm{s}} \omega_{\mathrm{k}} (\boldsymbol{i}_{\mathrm{s}}^k)^\top \boldsymbol{L}_{\mathrm{s}}^k \boldsymbol{J}^\top \boldsymbol{i}_{\mathrm{s}}^k \\ &\quad + \omega_{\mathrm{k}}^2 (\boldsymbol{i}_{\mathrm{s}}^k)^\top (\boldsymbol{L}_{\mathrm{s}}^k)^\top \boldsymbol{J}^\top \boldsymbol{J} \boldsymbol{\psi}_{\mathrm{pm}}^k + R_{\mathrm{s}} \omega_{\mathrm{k}} (\boldsymbol{\psi}_{\mathrm{pm}}^k)^\top \boldsymbol{J}^\top \boldsymbol{i}_{\mathrm{s}}^k + \omega_{\mathrm{k}}^2 (\boldsymbol{\psi}_{\mathrm{pm}}^k)^\top \boldsymbol{J}^\top \boldsymbol{J} \boldsymbol{L}_{\mathrm{s}}^k \boldsymbol{i}_{\mathrm{s}}^k + \omega_{\mathrm{k}}^2 \underbrace{(\boldsymbol{\psi}_{\mathrm{pm}}^k)^\top \boldsymbol{J}^\top \boldsymbol{J} \boldsymbol{\psi}_{\mathrm{pm}}^k}_{=\|\boldsymbol{\psi}_{\mathrm{pm}}^k\|^2 = \psi_{\mathrm{pm}}^2}. \end{aligned} \tag{14}$$

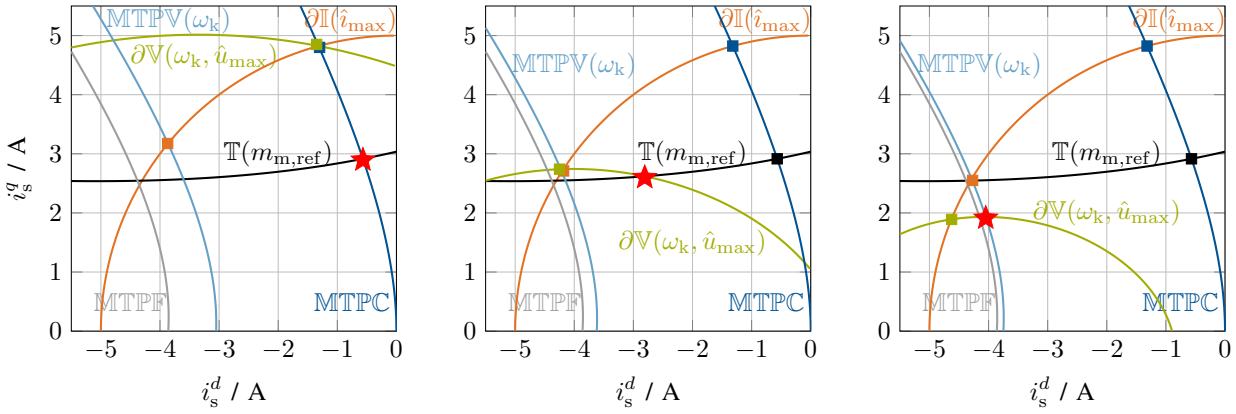

(a) *Maximum-Torque-per-Current (MTPC), i.e.,* $\mathbb{MTPC} \cap \mathbb{T}(m_{m,ref})$*, for* $\omega_k = \omega_{k,nom}^{MC} \leq \omega_{k,nom}$.

(b) *Field weakening (FW), i.e.,* $\mathbb{T}(m_{m,ref}) \cap \partial\mathbb{V}(\omega_k, \hat{u}_{max})$*, for* $\omega_{k,nom} < \omega_k = 2\omega_{k,nom} < \omega_{k,cut\text{-}in}^{MTPV}$.

(c) *Maximum-Torque-per-Voltage (MTPV), i.e.,* $\mathbb{MTPV}(\omega_k) \cap \partial\mathbb{V}(\omega_k, \hat{u}_{max})$*, for* $\omega_k = 3\omega_{k,nom} \geq \omega_{k,cut\text{-}in}^{MTPV}$ *($m_{m,ref}$ is not feasible anymore).*

Figure 3: *Illustration of three different feedforward torque control strategies for torque reference* $m_{m,ref} > 0$ *(2nd quadrant) and varying electrical angular velocities (a)* $\omega_k = \omega_{k,nom}$*, (b)* $\omega_k = 2\omega_{k,nom}$ *and (c)* $\omega_k = 3\omega_{k,nom}$*: The three plots show voltage ellipse* $\partial\mathbb{V}(\omega_k, \hat{u}_{max})$*, maximum current circle* $\partial\mathbb{I}(\hat{\imath}_{max})$*, MTPC hyperbola* $\mathbb{MTPC}$*, torque hyperbola* $\mathbb{T}(m_{m,ref})$*, MTPV hyperbola* $\mathbb{MTPV}(\omega_k)$*, MTPF hyperbola* $\mathbb{MTPF}$ *and optimal operation point* ★ *, respectively.*

To find a more compact representation, the goal is to rewrite (14) as a quadric. Therefore, in (14), terms of the form $(\boldsymbol{i}_s^k)^\top \square \boldsymbol{i}_s^k$ and $\square^\top \boldsymbol{i}_s^k$ (where $\square$ is either a matrix or a vector, respectively) are collected. Then, by defining

$$
\begin{aligned}
\boldsymbol{V}(\omega_k) &:= \begin{bmatrix} v_{11}(\omega_k), & v_{12}(\omega_k) \\ v_{12}(\omega_k), & v_{22}(\omega_k) \end{bmatrix} = R_s^2 \boldsymbol{I}_2 + R_s \omega_k \big(\boldsymbol{J} \boldsymbol{L}_s^k + \boldsymbol{L}_s^k \boldsymbol{J}^\top \big) + \omega_k^2 (\boldsymbol{L}_s^k)^2 \\
&= \begin{bmatrix} R_s^2 - 2\omega_k R_s L_m + \omega_k^2 [(L_s^d)^2 + L_m^2], & \omega_k R_s (L_s^d - L_s^q) + \omega_k^2 L_m (L_s^d + L_s^q) \\ \omega_k R_s (L_s^d - L_s^q) + \omega_k^2 L_m (L_s^d + L_s^q), & R_s^2 + 2\omega_k R_s L_m + \omega_k^2 [(L_s^q)^2 + L_m^2] \end{bmatrix} = \boldsymbol{V}(\omega_k)^\top, \\
\boldsymbol{v}(\omega_k)^\top &:= \begin{pmatrix} v_1(\omega_k) \\ v_2(\omega_k) \end{pmatrix} = \omega_k \, (\boldsymbol{\psi}_{pm}^k)^\top \big(\omega_k \boldsymbol{L}_s^k + R_s \boldsymbol{J}^\top \big) \overset{(2)}{=} \begin{cases} \begin{pmatrix} \omega_k^2 L_s^d \psi_{pm} \\ \omega_k \psi_{pm} (R_s + \omega_k L_m) \end{pmatrix}^\top, & \text{for PMSM or PME-RSM} \\ \begin{pmatrix} -\omega_k \psi_{pm} (R_s - \omega_k L_m) \\ \omega_k^2 L_s^q \psi_{pm} \end{pmatrix}^\top, & \text{for PMA-RSM} \\ (0,\, 0), & \text{for RSM} \end{cases} \\
\nu(\omega_k, \hat{u}_{max}) &:= \omega_k^2 \, (\boldsymbol{\psi}_{pm}^k)^\top \boldsymbol{J}^\top \boldsymbol{J} \boldsymbol{\psi}_{pm}^k - \hat{u}_{max}^2 \overset{(2)}{=} \begin{cases} \omega_k^2 \, \psi_{pm}^2 - \hat{u}_{max}^2, & \text{for PMSM, PME-RSM and PMA-RSM} \\ -\hat{u}_{max}^2, & \text{for RSM,} \end{cases}
\end{aligned}
\tag{15}
$$

the voltage constraint in (14) (or in (5)) can be expressed by

$$
\|\boldsymbol{u}_s^k\|^2 - \hat{u}_{max}^2 \overset{(14),(15)}{=} (\boldsymbol{i}_s^k)^\top \boldsymbol{V} \, \boldsymbol{i}_s^k + 2 \, \boldsymbol{v}^\top \boldsymbol{i}_s^k + \nu \leq 0.
$$

Finally, the voltage constraint (14) can be written implicitly as quadric surface defined by

$$
\mathbb{V}(\omega_k, \hat{u}_{max}) := \big\{ \, \boldsymbol{i}_s^k \in \mathbb{R}^2 \, \big| \, (\boldsymbol{i}_s^k)^\top \boldsymbol{V}(\omega_k) \, \boldsymbol{i}_s^k + 2 \, \boldsymbol{v}(\omega_k)^\top \boldsymbol{i}_s^k + \nu(\omega_k, \hat{u}_{max}) \leq 0 \big\}, \tag{16}
$$

which describes the *voltage elliptical area*. The *voltage ellipse* is given by

$$
\boxed{\partial\mathbb{V}(\omega_k, \hat{u}_{max}) := \big\{ \, \boldsymbol{i}_s^k \in \mathbb{R}^2 \, \big| \, \underbrace{(\boldsymbol{i}_s^k)^\top \boldsymbol{V}(\omega_k) \, \boldsymbol{i}_s^k + 2 \, \boldsymbol{v}(\omega_k)^\top \boldsymbol{i}_s^k + \nu(\omega_k, \hat{u}_{max})}_{=: Q_{\partial\mathbb{V}}(\boldsymbol{i}_s^k, \omega_k, \hat{u}_{max})} = 0 \big\},} \tag{17}
$$

i.e. the boundary of (16) (see —— line in Fig. 3). The quadric $Q_{\partial\mathbb{V}}(\boldsymbol{i}_s^k, \omega_k, \hat{u}_{max})$ of the voltage ellipse depends on currents $\boldsymbol{i}_s^k = (i_s^d, i_s^q)^\top$, angular velocity ω_k and voltage limit $\hat{u}_{max}$.

Remark III.2 (Speed dependency of the voltage ellipse and symmetry of $\boldsymbol{V}(\omega_k)$)**.** *Note that* $\boldsymbol{V}(\omega_k)$*,* $\boldsymbol{v}(\omega_k)$ *and* $\nu(\omega_k, \hat{u}_{max})$ *explicitly depend on the electrical angular velocity* ω_k*. Moreover, note that, the matrix* $\boldsymbol{V}(\omega_k) = \boldsymbol{V}(\omega_k)^\top \in \mathbb{R}^{2\times 2}$ *is* indeed

symmetric for all $\omega_\mathrm{k} \in \mathbb{R}$*, since all its sub-matrices are symmetric, respectively, i.e.* $(R_\mathrm{s}\boldsymbol{I}_2)^\top = R_\mathrm{s}\boldsymbol{I}_2$*,* $\left(\boldsymbol{J}\boldsymbol{L}_\mathrm{s}^k + \boldsymbol{L}_\mathrm{s}^k\boldsymbol{J}^\top\right)^\top = (\boldsymbol{J}\boldsymbol{L}_\mathrm{s}^k)^\top + (\boldsymbol{L}_\mathrm{s}^k\boldsymbol{J}^\top)^\top = \boldsymbol{L}_\mathrm{s}^k\boldsymbol{J}^\top + \boldsymbol{J}\boldsymbol{L}_\mathrm{s}^k = \begin{bmatrix} -2L_\mathrm{m} & L_\mathrm{s}^d - L_\mathrm{s}^q \\ L_\mathrm{s}^d - L_\mathrm{s}^q & 2L_\mathrm{m} \end{bmatrix}$ *and* $((\boldsymbol{L}_\mathrm{s}^k)^2)^\top = ((\boldsymbol{L}_\mathrm{s}^k)^\top\boldsymbol{L}_\mathrm{s}^k)^\top = (\boldsymbol{L}_\mathrm{s}^k)^\top\boldsymbol{L}_\mathrm{s}^k = (\boldsymbol{L}_\mathrm{s}^k)^2 = \begin{bmatrix} (L_\mathrm{s}^d)^2 + L_\mathrm{m}^2 & L_\mathrm{m}(L_\mathrm{s}^d + L_\mathrm{s}^q) \\ L_\mathrm{m}(L_\mathrm{s}^d + L_\mathrm{s}^q) & (L_\mathrm{s}^q)^2 + L_\mathrm{m}^2 \end{bmatrix}$.

3) Current circular area (reformulation of the current constraint in (5)*):* The current constraint in (5) can also be expressed implicitly as quadric as follows

$$\mathbb{I}(\hat{\imath}_\mathrm{max}) := \left\{\, \boldsymbol{i}_\mathrm{s}^k \in \mathbb{R}^2 \;\middle|\; (\boldsymbol{i}_\mathrm{s}^k)^\top \boldsymbol{I}_2 \boldsymbol{i}_\mathrm{s}^k - \hat{\imath}_\mathrm{max}^2 \leq 0 \,\right\} \tag{18}$$

which describes the admissible maximum current circular area: The magnitude of the stator current vector must not exceed the current limit $\hat{\imath}_\mathrm{max}$. The maximum current circle (see —— line in Fig. 3), i.e. the boundary of (18), is given by

$$\boxed{\partial\mathbb{I}(\hat{\imath}_\mathrm{max}) := \left\{\, \boldsymbol{i}_\mathrm{s}^k \in \mathbb{R}^2 \;\middle|\; (\boldsymbol{i}_\mathrm{s}^k)^\top \boldsymbol{I}_2 \boldsymbol{i}_\mathrm{s}^k - \hat{\imath}_\mathrm{max}^2 = 0 \,\right\}.} \tag{19}$$

Remark III.3 (Explicit expression for the maximum current circle)**.** *The current circle is given by* $i_\mathrm{s}^q = \pm\sqrt{\hat{\imath}_\mathrm{max}^2 - (i_\mathrm{s}^d)^2}$.

4) Flux norm: To operate the machine with the MTPF strategy, the (squared) norm of the flux linkage is minimized. It can also be expressed as quadric as follows

$$\|\boldsymbol{\psi}_\mathrm{pm}^k\|^2 \overset{(2)}{=} (\boldsymbol{L}_\mathrm{s}^k\boldsymbol{i}_\mathrm{s}^k + \boldsymbol{\psi}_\mathrm{pm}^k)^\top(\boldsymbol{L}_\mathrm{s}^k\boldsymbol{i}_\mathrm{s}^k + \boldsymbol{\psi}_\mathrm{pm}^k) =: \; (\boldsymbol{i}_\mathrm{s}^k)^\top\boldsymbol{F}\boldsymbol{i}_\mathrm{s}^k + 2\boldsymbol{f}\boldsymbol{i}_\mathrm{s}^k + \phi, \tag{20}$$

where

$$\left.\begin{aligned} \boldsymbol{F} \;&:=\; (\boldsymbol{L}_\mathrm{s}^k)^2 = \begin{bmatrix} (L_\mathrm{s}^d)^2 + L_\mathrm{m}^2 & L_\mathrm{m}(L_\mathrm{s}^d + L_\mathrm{s}^q) \\ L_\mathrm{m}(L_\mathrm{s}^d + L_\mathrm{s}^q) & (L_\mathrm{s}^q)^2 + L_\mathrm{m}^2 \end{bmatrix} = \boldsymbol{F}^\top, \\ \boldsymbol{f} \;&:=\; \boldsymbol{L}_\mathrm{s}^k\boldsymbol{\psi}_\mathrm{pm}^k \overset{(2)}{=} \begin{cases} \psi_\mathrm{pm}(L_\mathrm{s}^d,\, L_\mathrm{m})^\top, & \text{for PMSM and PME-RSM} \\ \psi_\mathrm{pm}(L_\mathrm{m},\, L_\mathrm{s}^q)^\top, & \text{for PMA-RSM} \\ (0,\, 0)^\top, & \text{for RSM,} \end{cases} \\ \phi \;&:=\; (\boldsymbol{\psi}_\mathrm{pm}^k)^\top\boldsymbol{\psi}_\mathrm{pm}^k = \|\boldsymbol{\psi}_\mathrm{pm}^k\|^2 = (\psi_\mathrm{pm}^d)^2 + (\psi_\mathrm{pm}^q)^2 \overset{(2)}{=} \begin{cases} \psi_\mathrm{pm}^2, & \text{for PMSM, PME-RSM and PMA-RSM} \\ 0, & \text{for RSM} \end{cases} \end{aligned}\right\} \tag{21}$$

are the corresponding matrix, vector and scalar of the flux linkage quadric.

IV. Operation strategies

In this section, the optimal operation strategies *Maximum Torque per Current (MTPC)*, *Maximum Current (MC)*, *Field Weakening (FW)*, *Maximum Torque per Voltage (MTPV)* and *Maximum Torque per Flux (MTPF)* are discussed in more detail and the analytical solutions of the respective reference currents are presented. Finally, the operation strategies are explained based on the visualization of the current loci (see Fig. 3). The significant impact of neglecting stator resistance and mutual inductance on the efficiency of the machine is illustrated (see Fig. 4) and discussed.

A. Maximum-Torque-per-Current (MTPC) hyperbola (considering L_m)

For low speeds, the voltage constraint in (5) is *not* critical. The current constraint in (5) and the minimization of (copper) losses dominate the operation of the machine which requires the use of the MTPC strategy (or mostly called Maximum-Torque-per-Ampere (MTPA) [34, Sec. 16.7.1] or [12], [17], [26]). The MTPC optimization problem is formulated as follows

$$\max_{\boldsymbol{i}_\mathrm{s}^k \in \mathbb{S}} -\|\boldsymbol{i}_\mathrm{s}^k\|^2 \quad \text{s.t.} \quad m_\mathrm{m}(\boldsymbol{i}_\mathrm{s}^k) = (\boldsymbol{i}_\mathrm{s}^k)^\top\boldsymbol{T}\boldsymbol{i}_\mathrm{s}^k + 2\boldsymbol{t}^\top(\boldsymbol{i}_\mathrm{s}^k) \overset{!}{=} m_\mathrm{m,ref}\big(\overset{(9)}{=} -\tau(m_\mathrm{m,ref})\big) \quad \text{with} \quad \mathbb{S} := \mathbb{V}(\omega_\mathrm{k}, \hat{u}_\mathrm{max}) \cap \mathbb{I}(\hat{\imath}_\mathrm{max}). \tag{22}$$

The admissible solution set $\mathbb{S}$ is the intersection of voltage elliptical area $\mathbb{V}(\omega_\mathrm{k}, \hat{u}_\mathrm{max})$ and current circular area $\mathbb{I}(\hat{\imath}_\mathrm{max})$. Its solution, the MTPC hyperbola (see —— line in Fig. 3), is given by the quadric

$$\boxed{\mathbb{MTPC} := \left\{\, \boldsymbol{i}_\mathrm{s}^k \in \mathbb{R}^2 \;\middle|\; (\boldsymbol{i}_\mathrm{s}^k)^\top \boldsymbol{M}_\mathrm{C}\, \boldsymbol{i}_\mathrm{s}^k + 2\,\boldsymbol{m}_\mathrm{C}^\top\boldsymbol{i}_\mathrm{s}^k = 0 \right\}} \tag{23}$$

where

$$\left.\begin{aligned} \boldsymbol{M}_{\mathrm{C}} &:= \tfrac{3}{2} n_{\mathrm{p}} \begin{bmatrix} \frac{L_{\mathrm{s}}^d - L_{\mathrm{s}}^q}{2} & L_{\mathrm{m}} \\ L_{\mathrm{m}}, & -\frac{L_{\mathrm{s}}^d - L_{\mathrm{s}}^q}{2} \end{bmatrix} = \boldsymbol{M}_{\mathrm{C}}^{\top} \qquad \text{and} \\ \boldsymbol{m}_{\mathrm{C}} &:= \tfrac{3}{2} n_{\mathrm{p}} \begin{pmatrix} \frac{\psi_{\mathrm{pm}}^d}{4} \\ \frac{\psi_{\mathrm{pm}}^q}{4} \end{pmatrix} \overset{(2)}{=} \begin{cases} \frac{3}{2} n_{\mathrm{p}} \left(\psi_{\mathrm{pm}},\, 0\right)^{\top}, & \text{for PMSM and PME-RSM} \\ \frac{3}{2} n_{\mathrm{p}} \left(0,\, \psi_{\mathrm{pm}}\right)^{\top}, & \text{for PMA-RSM} \\ (0,\, 0)^{\top}, & \text{for RSM.} \end{cases} \end{aligned}\right\} \tag{24}$$

The derivation of the implicit form (23) is presented in Appendix B. Note that the presented derivation can also be applied to obtain the implicit forms of MC, FW, MTPV and MTPF.

Remark IV.1 (Explicit expression for the MTPC hyperbola)**.** *Depending on the parameters L_{s}^d, L_{s}^q and L_{m}, the hyperbola can be expressed explicitly by*

$$\mathbb{MTPC}(i_{\mathrm{s}}^d) = \begin{cases} \dfrac{2L_{\mathrm{m}} i_{\mathrm{s}}^d + \frac{\psi_{\mathrm{pm}}^q}{2} \pm \sqrt{[(L_{\mathrm{s}}^d - L_{\mathrm{s}}^q)^2 + 4L_{\mathrm{m}}^2](i_{\mathrm{s}}^d)^2 + (2\psi_{\mathrm{pm}}^q L_{\mathrm{m}} + (L_{\mathrm{s}}^d - L_{\mathrm{s}}^q)\psi_{\mathrm{pm}}^d) i_{\mathrm{s}}^d + \frac{(\psi_{\mathrm{pm}}^q)^2}{4}}}{L_{\mathrm{s}}^d - L_{\mathrm{s}}^q} & \text{for } L_{\mathrm{s}}^d \neq L_{\mathrm{s}}^q \\ -(i_{\mathrm{s}}^d = 0), & \text{for } \; L_{\mathrm{s}}^d = L_{\mathrm{s}}^q, \end{cases} \tag{25}$$

which holds only for $i_{\mathrm{s}}^d \leq 0$ and $L_{\mathrm{s}}^q \geq L_{\mathrm{s}}^d$. For $i_{\mathrm{s}}^d > 0$ and/or $L_{\mathrm{s}}^d = L_{\mathrm{s}}^q$, another explicit expression has to be found. The implicit form (23) *with* (24) *holds in general (a significant advantage obviating the need of case studies). The mathematical derivation of the explicit expression of a general quadric is explained in Appendix C.*

Remark IV.2 (MTPC versus MTPA)**.** *In most publications, the MTPC strategy is called Maximum Torque Per Ampere (MTPA). From a physical point of view, the use of physical quantities in the terminology (like torque and current) seems more appropriate than a mixture of quantity and unit (like torque and Ampere). Therefore, in this paper, the terminology MTPC will be adopted instead of MTPA (following the publications [30], [39], [40]).*

B. Maximum current (MC)

To operate the machine at its current limit for increasing angular velocities, the MC strategy is used where the "optimal" reference currents are obtained as the intersection points of the current circle $\partial\mathbb{I}(\hat{\imath}_{\max})$ and the voltage ellipse $\partial\mathbb{V}(\omega_{\mathrm{k}}, \hat{u}_{\max})$. Hence, the reference current vectors are element of the following set

$$\boxed{\mathbb{MC}(\omega_{\mathrm{k}}, \hat{u}_{\max}, \hat{\imath}_{\max}) := \left\{ \boldsymbol{i}_{\mathrm{s}}^k \in \mathbb{R}^2 \;\middle|\; (\boldsymbol{i}_{\mathrm{s}}^k)^{\top} \boldsymbol{I}_2\, \boldsymbol{i}_{\mathrm{s}}^k - \hat{\imath}_{\max}^2 \overset{!}{=} (\boldsymbol{i}_{\mathrm{s}}^k)^{\top} \boldsymbol{V}(\omega_{\mathrm{k}}) \boldsymbol{i}_{\mathrm{s}}^k + 2\, \boldsymbol{v}(\omega_{\mathrm{k}})^{\top} \boldsymbol{i}_{\mathrm{s}}^k + \nu(\omega_{\mathrm{k}}, \hat{u}_{\max}) \right\}} \tag{26}$$

with $\boldsymbol{V}$, $\boldsymbol{v}$ and ν as in (15). An algorithm to compute these intersections points *analytically* is presented in Appendix D.

C. Field weakening (FW)

For a feasible torque below rated machine torque and angular velocities higher than a certain feasible MTPC velocity, the machine is operated in FW. The optimal reference currents are obtained by the intersection of the (feasible) torque hyperbola $\mathbb{T}(m_{\mathrm{m,ref}})$ and the voltage ellipse $\partial\mathbb{V}(\omega_{\mathrm{k}}, \hat{u}_{\max})$ and, hence, the reference current vector is element of the following set

$$\boxed{\mathbb{FW}(m_{\mathrm{m,ref}}, \omega_{\mathrm{k}}, \hat{u}_{\max}) := \left\{ \boldsymbol{i}_{\mathrm{s}}^k \in \mathbb{R}^2 \middle| (\boldsymbol{i}_{\mathrm{s}}^k)^{\top} \boldsymbol{T}\, \boldsymbol{i}_{\mathrm{s}}^k + 2\, \boldsymbol{t}^{\top} \boldsymbol{i}_{\mathrm{s}}^k + \tau(m_{\mathrm{m,ref}}) \overset{!}{=} (\boldsymbol{i}_{\mathrm{s}}^k)^{\top} \boldsymbol{V}(\omega_{\mathrm{k}}) \boldsymbol{i}_{\mathrm{s}}^k + 2\, \boldsymbol{v}(\omega_{\mathrm{k}})^{\top} \boldsymbol{i}_{\mathrm{s}}^k + \nu(\omega_{\mathrm{k}}, \hat{u}_{\max}) \right\}} \tag{27}$$

with $\boldsymbol{T}$, $\boldsymbol{t}$ and $\tau(m_{\mathrm{m,ref}})$ as in (9) and $\boldsymbol{V}(\omega_{\mathrm{k}})$, $\boldsymbol{v}(\omega_{\mathrm{k}})$ and $\nu(\omega_{\mathrm{k}}, \hat{u}_{\max})$ as in (15). Again, the computation of the intersection points is based on the analytical algorithm presented in Appendix D.

D. Maximum-Torque-per-Voltage (MTPV) hyperbola (considering R_{s} and L_{m})

For speeds higher than the MTPV cut-in speed $\omega_{\mathrm{k,cut\text{-}in}}^{\mathrm{MTPV}}$ and for torques higher than or equal to the speed-dependent MTPV cut-in torque $m_{\mathrm{m,cut\text{-}in}}^{\mathrm{MTPV}}$, the voltage constraint in (5) is critical and dominates the operation of the machine. The operation strategy now is MTPV. The corresponding MPTV optimization problem is formulated as follows

$$\max_{\boldsymbol{i}_{\mathrm{s}}^k \in \mathbb{S}} -\|\boldsymbol{u}_{\mathrm{s}}^k(\boldsymbol{i}_{\mathrm{s}}^k)\|^2 \quad \text{s.t.} \quad m_{\mathrm{m}}(\boldsymbol{i}_{\mathrm{s}}^k) = (\boldsymbol{i}_{\mathrm{s}}^k)^{\top} \boldsymbol{T} \boldsymbol{i}_{\mathrm{s}}^k + 2\boldsymbol{t}^{\top}(\boldsymbol{i}_{\mathrm{s}}^k) \overset{!}{=} m_{\mathrm{m,ref}} \quad \text{with} \quad \mathbb{S} = \mathbb{V}(\omega_{\mathrm{k}}, \hat{u}_{\max}) \cap \mathbb{I}(\hat{\imath}_{\max}). \tag{28}$$

Its solution, the MTPV hyperbola (see —— line in Fig. 3), is parametrized by the electrical angular velocity ω_{k} and is implicitly given by the quadric

$$\boxed{\mathbb{MTPV}(\omega_{\mathrm{k}}) := \left\{ \; \boldsymbol{i}_{\mathrm{s}}^k \in \mathbb{R}^2 \;\middle|\; (\boldsymbol{i}_{\mathrm{s}}^k)^{\top} \boldsymbol{M}_{\mathrm{V}}(\omega_{\mathrm{k}})\, \boldsymbol{i}_{\mathrm{s}}^k + 2\, \boldsymbol{m}_{\mathrm{V}}(\omega_{\mathrm{k}})^{\top} \boldsymbol{i}_{\mathrm{s}}^k + \mu_{\mathrm{V}}(\omega_{\mathrm{k}}) = 0 \right\}} \tag{29}$$

where

$$\left.\begin{aligned}
\boldsymbol{M}_{\mathrm{V}}(\omega_{\mathrm{k}}) &:= \begin{bmatrix} m_{\mathrm{V}}^{11}(\omega_{\mathrm{k}}), & m_{\mathrm{V}}^{12}(\omega_{\mathrm{k}}) \\ m_{\mathrm{V}}^{12}(\omega_{\mathrm{k}}), & m_{\mathrm{V}}^{22}(\omega_{\mathrm{k}}) \end{bmatrix} = \boldsymbol{M}_{\mathrm{V}}(\omega_{\mathrm{k}})^{\top} = \\
&= \tfrac{3}{2} n_{\mathrm{p}} \begin{bmatrix} \omega_{\mathrm{k}}^2 L_{\mathrm{m}}^2 (L_{\mathrm{s}}^d + L_{\mathrm{s}}^q) \\ \quad + \frac{L_{\mathrm{s}}^d - L_{\mathrm{s}}^q}{2} \Big(R_{\mathrm{s}}^2 + \omega_{\mathrm{k}}^2 \big[(L_{\mathrm{s}}^d)^2 + L_{\mathrm{m}}^2 \big] \Big) \end{bmatrix}, & \frac{L_{\mathrm{m}}}{2} \Big(2R_{\mathrm{s}}^2 + \omega_{\mathrm{k}}^2 \big[(L_{\mathrm{s}}^d)^2 + (L_{\mathrm{s}}^q)^2 + 2L_{\mathrm{m}}^2 \big] \Big) \\
\frac{L_{\mathrm{m}}}{2} \Big(2R_{\mathrm{s}}^2 + \omega_{\mathrm{k}}^2 \big[(L_{\mathrm{s}}^d)^2 + (L_{\mathrm{s}}^q)^2 + 2L_{\mathrm{m}}^2 \big] \Big), & \begin{bmatrix} \omega_{\mathrm{k}}^2 L_{\mathrm{m}}^2 (L_{\mathrm{s}}^d + L_{\mathrm{s}}^q) \\ - \frac{L_{\mathrm{s}}^d - L_{\mathrm{s}}^q}{2} \Big(R_{\mathrm{s}}^2 + \omega_{\mathrm{k}}^2 \big[(L_{\mathrm{s}}^q)^2 + L_{\mathrm{m}}^2 \big] \Big) \end{bmatrix} \end{bmatrix}, \\
\boldsymbol{m}_{\mathrm{V}}(\omega_{\mathrm{k}}) &:= \begin{pmatrix} m_{\mathrm{V}}^1(\omega_{\mathrm{k}}) \\ m_{\mathrm{V}}^2(\omega_{\mathrm{k}}) \end{pmatrix} = \tfrac{3}{2} n_{\mathrm{p}} \begin{pmatrix} \Big(R_{\mathrm{s}}^2 + \omega_{\mathrm{k}}^2 \big[2(L_{\mathrm{s}}^d)^2 - L_{\mathrm{s}}^q L_{\mathrm{s}}^d + 3L_{\mathrm{m}}^2 \big] \Big) \frac{\psi_{\mathrm{pm}}^d}{4} + \omega_{\mathrm{k}}^2 L_{\mathrm{m}} (L_{\mathrm{s}}^d + L_{\mathrm{s}}^q) \frac{\psi_{\mathrm{pm}}^q}{2} \\ \omega_{\mathrm{k}}^2 L_{\mathrm{m}} (L_{\mathrm{s}}^d + L_{\mathrm{s}}^q) \frac{\psi_{\mathrm{pm}}^d}{2} + \Big(R_{\mathrm{s}}^2 + \omega_{\mathrm{k}}^2 \big[2(L_{\mathrm{s}}^d)^2 - L_{\mathrm{s}}^q L_{\mathrm{s}}^d + 3L_{\mathrm{m}}^2 \big] \Big) \frac{\psi_{\mathrm{pm}}^q}{4} \end{pmatrix} \quad \text{and} \\
\mu_{\mathrm{V}}(\omega_{\mathrm{k}}) &:= \tfrac{3}{4} n_{\mathrm{p}} \omega_{\mathrm{k}}^2 \Big[L_{\mathrm{s}}^d (\psi_{\mathrm{pm}}^d)^2 + 2L_{\mathrm{m}} \psi_{\mathrm{pm}}^d \psi_{\mathrm{pm}}^q + L_{\mathrm{s}}^q (\psi_{\mathrm{pm}}^q)^2 \Big] \overset{(2)}{=} \begin{cases} \frac{3}{4} n_{\mathrm{p}} \omega_{\mathrm{k}}^2 L_{\mathrm{s}}^d \psi_{\mathrm{pm}}^2, & \text{for PMSM and PME-RSM} \\ \frac{3}{4} n_{\mathrm{p}} \omega_{\mathrm{k}}^2 L_{\mathrm{s}}^q \psi_{\mathrm{pm}}^2, & \text{for PMA-RSM} \\ 0, & \text{for RSM.} \end{cases}
\end{aligned}\right\} \tag{30}$$

Obviously, since $\boldsymbol{M}_{\mathrm{V}}(\omega_{\mathrm{k}})$, $\boldsymbol{m}_{\mathrm{V}}(\omega_{\mathrm{k}})$ and $\mu_{\mathrm{V}}(\omega_{\mathrm{k}})$ *all* depend on the angular velocity ω_{k}, the MTPV hyperbola is moving in the $(i_{\mathrm{s}}^d, i_{\mathrm{s}}^q)$-plane (see —— lines in Fig. 3(a), (b) & (c)).

Remark IV.3 (Explicit expression for the MTPV hyperbola)**.** *The explicit solution of the MTPV hyperbola is given by (see Appendix C)*

$$\mathbb{MTPV}(i_{\mathrm{s}}^d, \omega_{\mathrm{k}}) = -\frac{m_{\mathrm{V}}^{12}\, i_{\mathrm{s}}^d + m_{\mathrm{V}}^2}{m_{\mathrm{V}}^{22}} \pm \frac{\sqrt{\Big(m_{\mathrm{V}}^{12}\, i_{\mathrm{s}}^d + m_{\mathrm{V}}^2 \Big)^2 - m_{\mathrm{V}}^{22} \Big(m_{\mathrm{V}}^{11}\, (i_{\mathrm{s}}^d)^2 + 2 m_{\mathrm{V}}^1\, i_{\mathrm{s}}^d + \mu_{\mathrm{V}} \Big)}}{m_{\mathrm{V}}^{22}}, \tag{31}$$

where $m_{\mathrm{V}}^{11} = m_{\mathrm{V}}^{11}(\omega_{\mathrm{k}})$, $m_{\mathrm{V}}^{12} = m_{\mathrm{V}}^{12}(\omega_{\mathrm{k}})$, $m_{\mathrm{V}}^{22} = m_{\mathrm{V}}^{22}(\omega_{\mathrm{k}})$, $m_{\mathrm{V}}^{1} = m_{\mathrm{V}}^{1}(\omega_{\mathrm{k}})$, $m_{\mathrm{V}}^{2} = m_{\mathrm{V}}^{2}(\omega_{\mathrm{k}})$ *and* $\mu_{\mathrm{V}} = \mu_{\mathrm{V}}(\omega_{\mathrm{k}})$ *are as in* (30)*. Note that* $m_{\mathrm{V}}^{22}(0) = -\frac{L_{\mathrm{s}}^d - L_{\mathrm{s}}^q}{2} R_{\mathrm{s}}^2 \neq 0$ *and, hence, is non-zero for all* ω_{k} *and all* $L_{\mathrm{s}}^d \neq L_{\mathrm{s}}^q$*.*

Remark IV.4 (MTPV hyperbola without stator resistance)**.** *Note that the MTPV hyperbola without stator resistance can be obtained from* (30) *by setting* $R_{\mathrm{s}} = 0$*. This was already shown in [30].*

E. Maximum-Torque-per-Flux (MTPF) hyperbola (considering L_{m})

For high speeds, an alternative to the MTPV strategy is the MTPF strategy. Nevertheless, it yields a reference current vector with larger magnitude than that obtained from MTPV; hence, the MTPV strategy should be used instead (see also Remark IV.6). The MTPF optimization problem can be formulated as follows

$$\max_{\boldsymbol{i}_{\mathrm{s}}^k \in \mathbb{S}} -\|\boldsymbol{\psi}_{\mathrm{s}}^k(\boldsymbol{i}_{\mathrm{s}}^k)\|^2 \quad \text{s.t.} \quad m_{\mathrm{m}}(\boldsymbol{i}_{\mathrm{s}}^k) = (\boldsymbol{i}_{\mathrm{s}}^k)^{\top} \boldsymbol{T} \boldsymbol{i}_{\mathrm{s}}^k + 2\boldsymbol{t}^{\top}(\boldsymbol{i}_{\mathrm{s}}^k) \overset{!}{=} m_{\mathrm{m,ref}} \quad \text{with} \quad \mathbb{S} := \mathbb{V}(\omega_{\mathrm{k}}, \hat{u}_{\max}) \cap \mathbb{I}(\hat{\imath}_{\max}). \tag{32}$$

Its solution, the MTPF hyperbola (see —— line in Fig. 3) is implicitly given by the quadric

$$\boxed{\mathbb{MTPF} := \big\{ \boldsymbol{i}_{\mathrm{s}}^k \in \mathbb{R}^2 \;\big|\; (\boldsymbol{i}_{\mathrm{s}}^k)^{\top} \boldsymbol{M}_{\mathrm{F}}\, \boldsymbol{i}_{\mathrm{s}}^k + 2\, \boldsymbol{m}_{\mathrm{F}}^{\top} \boldsymbol{i}_{\mathrm{s}}^k + \mu_{\mathrm{F}} = 0 \big\},} \tag{33}$$

which does *not* depend on the angular velocity ω_{k} (in contrast to the MTPV hyperbola), since

$$\left.\begin{aligned}
\boldsymbol{M}_{\mathrm{F}} &:= \begin{bmatrix} m_{\mathrm{F}}^{11}, & m_{\mathrm{F}}^{12} \\ m_{\mathrm{F}}^{12}, & m_{\mathrm{F}}^{22} \end{bmatrix} = \boldsymbol{M}_{\mathrm{F}}^{\top} = \\
&= \tfrac{3}{2} n_{\mathrm{p}} \begin{bmatrix} \frac{L_{\mathrm{s}}^d - L_{\mathrm{s}}^q}{2} \big((L_{\mathrm{s}}^d)^2 + L_{\mathrm{m}}^2 \big) + L_{\mathrm{m}}^2 \big(L_{\mathrm{s}}^d + L_{\mathrm{s}}^q \big), & \frac{L_{\mathrm{m}}}{2} \big((L_{\mathrm{s}}^d)^2 + (L_{\mathrm{s}}^q)^2 + 2L_{\mathrm{m}}^2 \big) \\ \frac{L_{\mathrm{m}}}{2} \big((L_{\mathrm{s}}^d)^2 + (L_{\mathrm{s}}^q)^2 + 2L_{\mathrm{m}}^2 \big), & - \frac{L_{\mathrm{s}}^d - L_{\mathrm{s}}^q}{2} \big((L_{\mathrm{s}}^q)^2 + L_{\mathrm{m}}^2 \big) + L_{\mathrm{m}}^2 \big(L_{\mathrm{s}}^d + L_{\mathrm{s}}^q \big) \end{bmatrix}, \\
\boldsymbol{m}_{\mathrm{F}} &:= \begin{pmatrix} m_{\mathrm{F}}^1 \\ m_{\mathrm{F}}^2 \end{pmatrix} = \tfrac{3}{2} n_{\mathrm{p}} \begin{pmatrix} \Big(2(L_{\mathrm{s}}^d)^2 - L_{\mathrm{s}}^d L_{\mathrm{s}}^q + 3L_{\mathrm{m}}^2 \Big) \frac{\psi_{\mathrm{pm}}^d}{4} + L_{\mathrm{m}} (L_{\mathrm{s}}^d + L_{\mathrm{s}}^q) \frac{\psi_{\mathrm{pm}}^q}{2} \\ L_{\mathrm{m}} (L_{\mathrm{s}}^d + L_{\mathrm{s}}^q) \frac{\psi_{\mathrm{pm}}^d}{2} + \Big(2(L_{\mathrm{s}}^q)^2 - L_{\mathrm{s}}^d L_{\mathrm{s}}^q + 3L_{\mathrm{m}}^2 \Big) \frac{\psi_{\mathrm{pm}}^q}{4} \end{pmatrix} \quad \text{and} \\
\mu_{\mathrm{F}} &:= \tfrac{3}{4} n_{\mathrm{p}} \Big[L_{\mathrm{s}}^d (\psi_{\mathrm{pm}}^d)^2 + 2L_{\mathrm{m}} \psi_{\mathrm{pm}}^d \psi_{\mathrm{pm}}^q + L_{\mathrm{s}}^q (\psi_{\mathrm{pm}}^q)^2 \Big] \overset{(2)}{=} \begin{cases} \frac{3}{4} n_{\mathrm{p}} L_{\mathrm{s}}^d (\psi_{\mathrm{pm}})^2, & \text{for PMSM and PME-RSM} \\ \frac{3}{4} n_{\mathrm{p}} L_{\mathrm{s}}^q (\psi_{\mathrm{pm}})^2, & \text{for PMA-RSM} \\ 0, & \text{for RSM,} \end{cases}
\end{aligned}\right\} \tag{34}$$

strategy	current reference vector	algorithm used
MTPC	$\boldsymbol{i}_{\mathrm{s,ref}}^{k,\mathrm{MTPC}}(\lambda^\star) \overset{(50)}{:=} -\big[\lambda^\star \boldsymbol{T} - \boldsymbol{I}_2\big]^{-1}\lambda^\star \boldsymbol{t}$	see Appendix A where $\boldsymbol{A}=\boldsymbol{I}_2$, $\boldsymbol{a}=\boldsymbol{0}_2$, $\boldsymbol{B}=\boldsymbol{T}$ & $\boldsymbol{b}=\boldsymbol{t}$
MC	$\boldsymbol{i}_{\mathrm{s,ref}}^{k,\mathrm{MC}}(\gamma^\star) \overset{(68)}{:=} -\big[\big(\frac{\boldsymbol{I}_2}{-\hat{\imath}_{\max}^2} - \frac{\boldsymbol{V}(\omega_\mathrm{k})}{\nu(\omega_\mathrm{k},\hat{u}_{\max})}\big) - \gamma^\star \boldsymbol{J}\big]^{-1}\frac{2\boldsymbol{v}(\omega_\mathrm{k})}{\nu(\omega_\mathrm{k},\hat{u}_{\max})}$	see Appendix D (case (i)) where $\boldsymbol{A}=\boldsymbol{I}_2$, $\boldsymbol{a}=\boldsymbol{0}_2$, $\alpha=-\hat{\imath}_{\max}^2$, $\boldsymbol{B}=\boldsymbol{V}(\omega_\mathrm{k})$, $\boldsymbol{b}=\boldsymbol{v}(\omega_\mathrm{k})$, $\beta=\nu(\omega_\mathrm{k},\hat{u}_{\max})$, $\boldsymbol{D}=\big(\frac{\boldsymbol{A}}{\alpha}-\frac{\boldsymbol{B}}{\beta}\big)$ & $\boldsymbol{d}=\big(\frac{\boldsymbol{a}}{\alpha}-\frac{\boldsymbol{b}}{\beta}\big)$
FW	$\boldsymbol{i}_{\mathrm{s,ref}}^{k,\mathrm{FW}}(\gamma^\star) \overset{(68)}{:=} -2\big[\boldsymbol{D} - \gamma^\star \boldsymbol{J}\big]^{-1}\boldsymbol{d}$	see Appendix D (case (i)) where $\boldsymbol{A}=\boldsymbol{T}$, $\boldsymbol{a}=\boldsymbol{t}$, $\alpha=\tau(m_{\mathrm{m,ref}})$, $\boldsymbol{B}=\boldsymbol{V}(\omega_\mathrm{k})$, $\boldsymbol{b}=\boldsymbol{v}(\omega_\mathrm{k})$, $\beta=\nu(\omega_\mathrm{k},\hat{u}_{\max})$, $\boldsymbol{D}=\big(\frac{\boldsymbol{A}}{\alpha}-\frac{\boldsymbol{B}}{\beta}\big)$ & $\boldsymbol{d}=\big(\frac{\boldsymbol{a}}{\alpha}-\frac{\boldsymbol{b}}{\beta}\big)$
MTPF	$\boldsymbol{i}_{\mathrm{s,ref}}^{k,\mathrm{MTPF}}(\lambda^\star) \overset{(50)}{:=} -\big[\lambda^\star \boldsymbol{T} - \boldsymbol{F}\big]^{-1}\big(\lambda^\star \boldsymbol{t} - \boldsymbol{f}\big)$	see Appendix A where $\boldsymbol{A}=\boldsymbol{F}$, $\boldsymbol{a}=\boldsymbol{f}$, $\boldsymbol{B}=\boldsymbol{T}$ & $\boldsymbol{b}=\boldsymbol{t}$
MTPV	$\boldsymbol{i}_{\mathrm{s,ref}}^{k,\mathrm{MTPV}}(\lambda^\star) \overset{(50)}{:=} -\big[\lambda^\star \boldsymbol{T} - \boldsymbol{V}(\omega_\mathrm{k})\big]^{-1}\big(\lambda^\star \boldsymbol{t} - \boldsymbol{v}(\omega_\mathrm{k})\big)$	see Appendix A where $\boldsymbol{A}=\boldsymbol{V}(\omega_\mathrm{k})$, $\boldsymbol{a}=\boldsymbol{v}(\omega_\mathrm{k})$, $\boldsymbol{B}=\boldsymbol{T}$ & $\boldsymbol{b}=\boldsymbol{t}$

Table I: *Collection of the analytical solutions of the (optimal) current reference vectors for all operation strategies.*

do *not* depend on the electrical angular velocity ω_k, respectively.

Remark IV.5 (Explicit expression for the MTPF hyperbola)**.** *The explicit solution of the MTPF hyperbola is given by (see Appendix C)*

$$\mathbb{MTPF}(i_\mathrm{s}^d) = -\frac{m_\mathrm{F}^{12}\, i_\mathrm{s}^d + m_\mathrm{F}^2}{m_\mathrm{F}^{22}} \pm \frac{\sqrt{\Big(m_\mathrm{F}^{12}\, i_\mathrm{s}^d + m_\mathrm{F}^2\Big)^2 - m_\mathrm{F}^{22}\Big(m_\mathrm{F}^{11}\,(i_\mathrm{s}^d)^2 + 2m_\mathrm{F}^1\, i_\mathrm{s}^d + \mu_\mathrm{F}\Big)}}{m_\mathrm{F}^{22}}, \tag{35}$$

where m_F^{11}, m_F^{12}, m_F^{22}, m_F^1, m_F^2 *and* μ_F *are as in* (34)*. Note that* $m_\mathrm{F}^{22} = \frac{3}{2}n_\mathrm{p}\big[-\frac{L_\mathrm{s}^d - L_\mathrm{s}^q}{2}\big((L_\mathrm{s}^q)^2 + L_\mathrm{m}^2\big) + L_\mathrm{m}^2\big(L_\mathrm{s}^d + L_\mathrm{s}^q\big)\big] \neq 0$.

Remark IV.6 (Convergence of the MTPV hyperbola to the MTPF hyperbola)**.** *For very large electrical angular velocities* $|\omega_\mathrm{k}| \gg 1$ *or very small stator resistances* $R_\mathrm{s} \ll 1\,\Omega$*, the MTPV hyperbola converges to the shape of the MTPF hyperbola, since, either for* $\omega_\mathrm{k} \to \infty$ *or for* $R_\mathrm{s} = 0$*, the following holds*

$$(\boldsymbol{i}_\mathrm{s}^k)^\top \boldsymbol{M}_\mathrm{F}\, \boldsymbol{i}_\mathrm{s}^k + 2\,\boldsymbol{m}_\mathrm{F}^\top \boldsymbol{i}_\mathrm{s}^k + \mu_\mathrm{F} = 0 = \begin{cases} \lim\limits_{\omega_\mathrm{k}\to\infty} (\boldsymbol{i}_\mathrm{s}^k)^\top \frac{\boldsymbol{M}_\mathrm{V}(\omega_\mathrm{k})}{\omega_\mathrm{k}^2}\, \boldsymbol{i}_\mathrm{s}^k + 2\,\frac{\boldsymbol{m}_\mathrm{V}(\omega_\mathrm{k})^\top}{\omega_\mathrm{k}^2}\boldsymbol{i}_\mathrm{s}^k + \frac{\mu_\mathrm{V}(\omega_\mathrm{k})}{\omega_\mathrm{k}^2}, & R_\mathrm{s} \neq 0 \\ (\boldsymbol{i}_\mathrm{s}^k)^\top \frac{\boldsymbol{M}_\mathrm{V}(\omega_\mathrm{k})}{\omega_\mathrm{k}^2}\, \boldsymbol{i}_\mathrm{s}^k + 2\,\frac{\boldsymbol{m}_\mathrm{V}(\omega_\mathrm{k})^\top}{\omega_\mathrm{k}^2}\boldsymbol{i}_\mathrm{s}^k + \frac{\mu_\mathrm{V}(\omega_\mathrm{k})}{\omega_\mathrm{k}^2}, & R_\mathrm{s} = 0. \end{cases},$$

Concluding, only *for very large speeds or very small value of the stator resistance, both strategies are similar. In general, MTPF and MTPV hyperbola are* different *solutions to different optimization problems and give different optimal reference currents (see Fig. 3c).*

F. Analytical solutions of the optimal reference current vector for MTPC, MC, FW, MTPV and MTPF

In Tab. I, for each operation strategy, the analytical expression for the (optimal) current reference vector $\boldsymbol{i}_{\mathrm{s,ref}}^k = \boldsymbol{i}_{\mathrm{s,ref}}^{k,\mathrm{X}}$, $\mathrm{X} \in \{\mathrm{MTPC, MC, FW, MTPV, MTPF}\}$ and the used computation method (algorithm) are listed in compact form. In all cases, $\lambda^\star$ and $\gamma^\star$ are the optimal Lagrangian multipliers which represent one of the (real) roots of the polynomial (45) and (66), respectively. The four roots can be computed analytically by the algorithm presented in Appendix A3 (Euler's solution [41]).

Remark IV.7 (Alternative computation of optimal reference currents for MTPC, MTPV and MTPF)**.** *Note that, alternatively, by using the algorithm discussed in Appendix D, the optimal current reference vectors for MTPC, MTPF or MTPV can also be obtained by computing the intersection points of torque hyperbola* (12) *and MTPC hyperbola* (23)*, MTPV hyperbola* (29) *or MTPF hyperbola* (33)*, respectively.*

G. Graphical illustration of the operation strategies MPTC, FW and MTPV

In Fig. 3, for a 400 W synchronous machine with the following parameters

$$R_\mathrm{s} = 20\,\Omega,\ L_\mathrm{s}^d = 6\cdot 10^{-2}\,\mathrm{H},\ L_\mathrm{s}^q = 8\cdot 10^{-2}\,\mathrm{H}, L_\mathrm{m} = 0.5\cdot 10^{-3}\,\mathrm{H}, \boldsymbol{\psi}_\mathrm{pm}^k = (\psi_\mathrm{pm},\,0)^\top = (0.23\,\mathrm{Wb},\,0)^\top \text{ and } n_\mathrm{p} = 3, \tag{36}$$

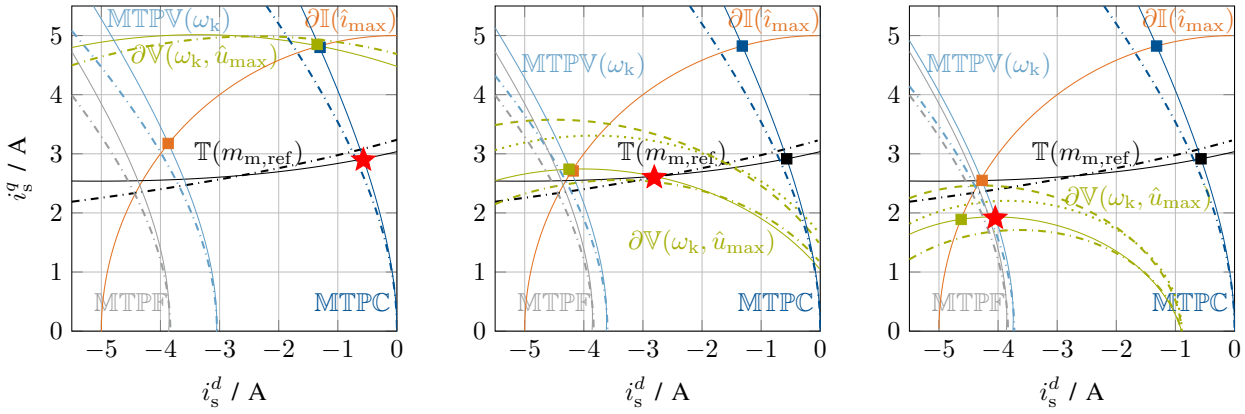

(a) *Maximum-Torque-per-Current (MTPC), i.e.,* $\mathbb{MTPC} \cap \mathbb{T}(m_{\mathrm{m,ref}})$*, for* $\omega_k = \omega_{k,nom} \leq \omega_{k,nom}$.

(b) *Field weakening (FW), i.e.,* $\mathbb{T}(m_{\mathrm{m,ref}}) \cap \partial\mathbb{V}(\omega_k, \hat{u}_{max})$*, for* $\omega_{k,nom} < \omega_k = 2\omega_{k,nom} < \omega_{k,cut\text{-}in}^{MTPV}$.

(c) *Maximum-Torque-per-Voltage (MTPV), i.e.,* $\mathbb{MTPV}(\omega_k) \cap \partial\mathbb{V}(\omega_k, \hat{u}_{max})$*, for* $\omega_k = 3\omega_{k,nom} \geq \omega_{k,cut\text{-}in}^{MTPV}$ *(*$m_{m,ref}$ *is* not *feasible anymore).*

Figure 4: *Illustration of the impact of* neglecting *stator resistance (dashed line:* $R_s = 0$*), mutual inductance (dash-dotted:* $L_m = 0$*) or both (dotted:* $R_s = L_m = 0$*)) on the different feedforward torque control strategies from Fig. 3: The three plots show voltage ellipse* $\partial\mathbb{V}(\omega_k, \hat{u}_{max})$*,* $\partial\mathbb{V}(\omega_k, \hat{u}_{max}; R_s = 0)$*,* $\partial\mathbb{V}(\omega_k, \hat{u}_{max}; L_m = 0)$*,* $\partial\mathbb{V}(\omega_k, \hat{u}_{max}; R_s = L_m = 0)$*, maximum current circle* $\partial\mathbb{I}(\hat{\imath}_{max})$*, MTPC hyperbola* $\mathbb{MTPC}$*,* $\mathbb{MTPC}(L_m = 0)$*, torque hyperbola* $\mathbb{T}(m_{m,ref})$*,* $\mathbb{T}(m_{m,ref}; L_m = 0)$*, MTPV hyperbola* $\mathbb{MTPV}(\omega_k)$*,* $\mathbb{MTPV}(\omega_k; L_m = 0)$*, MTPF hyperbola* $\mathbb{MTPF}$*,* $\mathbb{MTPF}(L_m = 0)$ *and optimal operation point* ★ *, respectively.*

three different optimal feedforward torque control strategies are illustrated for positive reference torque $m_{m,ref} = 3.35\,\mathrm{N\,m}$, voltage limit $\hat{u}_{max} = 600\,\mathrm{V}$ and current limit $\hat{\imath}_{max} = 5\,\mathrm{A}$. The illustrated optimal operation strategies are MTPC in Fig. 3a, FW in Fig. 3b, and MTPV in Fig. 3c. The respective optimal operation point, with its optimal reference current vector $\boldsymbol{i}_{s,ref}^k = (i_{s,ref}^d, i_{s,ref}^q)^\top$, is marked by ★ and corresponds to the intersection of (a) $\mathbb{MTPC} \cap \mathbb{T}(m_{m,ref})$ for MTPC in Fig. 3a, (b) $\partial\mathbb{V}(\omega_k, \hat{u}_{max}) \cap \mathbb{T}(m_{m,ref})$ for FW in Fig. 3b, and (c) $\mathbb{MTPV} \cap \partial\mathbb{V}(\omega_k, \hat{u}_{max})$ for MTPV in Fig. 3c.

For increasing electrical angular velocities $\omega_k \in \{1, 2, 3\}\omega_{k,nom}$ (where $\omega_{k,nom}$ is the nominal angular velocity), the MTPV hyperbola is approaching the MTPF hyperbola (recall Remark IV.6) and the voltage ellipse is shrinking; whereas the current circle, MTPC hyperbola, torque hyperbola and MTPF hyperbola are independent of the angular velocity and, hence, do *not* change in the three plots. The blue square represents the intersection of the MTPC hyperbola with the current circle and gives the nominal current vector $\boldsymbol{i}_{s,nom}^k$ producing the nominal torque $m_{m,nom}(\boldsymbol{i}_{s,nom}^k)$. The orange square highlights the intersection of current circle and torque hyperbola (in the 2^{nd} quadrant) and represents the maximally feasible current and maximally feasible torque for higher angular velocities.

Fig. 4 illustrates the impact of neglecting (i) stator resistance (i.e. $R_s = 0$: dashed line), (ii) mutual inductance (i.e. $L_m = 0$: dash-dotted line) or (iii) both (i.e. $R_s = L_m = 0$: dotted line) on the shape of MTPC, MTPV, MTPF and torque hyperbolas and the voltage ellipse. The feedforward torque control strategies and optimal operation points (marked by ★) are identical to those shown in Fig. 3. It is easy to see that neglecting stator resistance, mutual inductance or both will lead to completely different (and wrong) intersection points and, hence, *not* optimal operation points with *reduced efficiency*. For example, the impact of neglecting stator resistance, mutual inductance or both on the shape, size and orientation of the voltage ellipse is obvious. Concluding, for optimal operation of a synchronous machine, both parameters must *not* be neglected.

In Fig. 3 and 4, the intersection points of (a) current circle and MTPC hyperbola, (b) current circle and MTPV hyperbola, (c) current circle and voltage ellipse, and (d) torque and MTPC hyperbola are highlighted by the following colored squares (a) ■, (b) ■, (c) ■, and (d) ■, respectively.

ACKNOWLEDGEMENT

This project has received funding from the European Union's Horizon 2020 research and innovation programme under the Marie Sklodowska-Curie grant agreement No. 642682 and from the Bavarian Ministry for Eduction, Culture, Science, and Art.

APPENDIX

In this appendix, all necessary mathematical derivations are presented for two general quadrics given by

$$Q_A(\boldsymbol{x}) := \boldsymbol{x}^\top \boldsymbol{A}\boldsymbol{x} + 2\boldsymbol{a}^\top \boldsymbol{x} + \alpha \qquad \text{and} \qquad Q_B(\boldsymbol{x}) := \boldsymbol{x}^\top \boldsymbol{B}\boldsymbol{x} + 2\boldsymbol{b}^\top \boldsymbol{x} + \beta, \tag{37}$$

where

$$\boldsymbol{A}=\boldsymbol{A}^{\top}:=\begin{bmatrix}a_{11} & a_{12}\\ a_{12} & a_{22}\end{bmatrix}\in\mathbb{R}^{2\times 2},\ \boldsymbol{a}:=\begin{pmatrix}a_1\\ a_2\end{pmatrix}\in\mathbb{R}^2,\ \alpha\in\mathbb{R},\ \boldsymbol{B}=\boldsymbol{B}^{\top}:=\begin{bmatrix}b_{11} & b_{12}\\ b_{12} & b_{22}\end{bmatrix}\in\mathbb{R}^{2\times 2},\ \boldsymbol{b}:=\begin{pmatrix}b_1\\ b_2\end{pmatrix}\in\mathbb{R}^2 \text{ and } \beta\in\mathbb{R}. \tag{38}$$

Main goal is to explain in detail how analytical solutions to the MTPC, MTPV and MTPF optimization problems can be obtained and how analytical solutions for the intersection points of two general quadrics can be found. As it will be shown, all problems can be solved by finding the roots of a fourth-order *quartic polynomial* for which (luckily) still an analytical solutions exists.

A. Formulation of the optimization problem with equality constraints

All optimization problems like MTPC, MTPV and MTPF can be formulated in a general framework as optimization problems with equality constraint by invoking the quadrics $Q_A(\boldsymbol{i}_{\mathrm{s}}^k)$ and $Q_B(\boldsymbol{i}_{\mathrm{s}}^k)$ in (37) as follows

$$\boldsymbol{i}_{\mathrm{s,ref}}^k:=\arg\max\nolimits_{\boldsymbol{i}_{\mathrm{s}}^k}-\Big(\underbrace{(\boldsymbol{i}_{\mathrm{s}}^k)^{\top}\boldsymbol{A}\boldsymbol{i}_{\mathrm{s}}^k+2\boldsymbol{a}^{\top}\boldsymbol{i}_{\mathrm{s}}^k+\alpha}_{=:Q_A(\boldsymbol{i}_{\mathrm{s}}^k)}\Big)\qquad\text{s.t.}\qquad\underbrace{(\boldsymbol{i}_{\mathrm{s}}^k)^{\top}\boldsymbol{B}\boldsymbol{i}_{\mathrm{s}}^k+2\boldsymbol{b}^{\top}\boldsymbol{i}_{\mathrm{s}}^k+\beta}_{=:Q_B(\boldsymbol{i}_{\mathrm{s}}^k)}=0. \tag{39}$$

A first idea, based on quadrics, was presented in [42] for the MTPC strategy. The optimization problem (39) can be reformulated as *Lagrangian* (see [43, Cha. 5]) where the (possibly complex) Lagrangian multiplier $\lambda\in\mathbb{C}$ must be introduced for the equality constraint, i.e.

$$\mathfrak{L}(\boldsymbol{i}_{\mathrm{s}}^k,\lambda):=-Q_A(\boldsymbol{i}_{\mathrm{s}}^k)+\lambda\,Q_B(\boldsymbol{i}_{\mathrm{s}}^k)\overset{(39)}{=}-\big[(\boldsymbol{i}_{\mathrm{s}}^k)^{\top}\boldsymbol{A}\boldsymbol{i}_{\mathrm{s}}^k+2\boldsymbol{a}^{\top}\boldsymbol{i}_{\mathrm{s}}^k+\alpha\big]+\lambda\,\big[(\boldsymbol{i}_{\mathrm{s}}^k)^{\top}\boldsymbol{B}\boldsymbol{i}_{\mathrm{s}}^k+2\boldsymbol{b}^{\top}\boldsymbol{i}_{\mathrm{s}}^k+\beta\big]. \tag{40}$$

For the three different optimization problems MTPC, MTPF and MTPV, the matrices $\boldsymbol{A}$, $\boldsymbol{B}$, the vectors $\boldsymbol{a}$, $\boldsymbol{b}$ and the scalars α, β must be chosen properly according to the considered optimization problem as specified in the following:

- MTPC: $\boldsymbol{A}=\boldsymbol{I}_2$, $\boldsymbol{a}=(0,\,0)^{\top}$, $\alpha=0$ and $\boldsymbol{B}=\boldsymbol{T}$, $\boldsymbol{b}=\boldsymbol{t}$ and $\beta=\tau(m_{\mathrm{m,ref}})$,
- MTPV: $\boldsymbol{A}=\boldsymbol{V}(\omega_{\mathrm{k}})$, $\boldsymbol{a}=\boldsymbol{v}(\omega_{\mathrm{k}})$, $\alpha=\nu(\omega_{\mathrm{k}},\hat{u}_{\max})$ and $\boldsymbol{B}=\boldsymbol{T}$, $\boldsymbol{b}=\boldsymbol{t}$ and $\beta=\tau(m_{\mathrm{m,ref}})$, and
- MTPF: $\boldsymbol{A}=\boldsymbol{F}$, $\boldsymbol{a}=\boldsymbol{f}$, $\alpha=\phi$ and $\boldsymbol{B}=\boldsymbol{T}$, $\boldsymbol{b}=\boldsymbol{t}$ and $\beta=\tau(m_{\mathrm{m,ref}})$,

with $\boldsymbol{T}$, $\boldsymbol{t}$ and $\tau(m_{\mathrm{m,ref}})$ as in (9), $\boldsymbol{V}(\omega_{\mathrm{k}})$, $\boldsymbol{v}(\omega_{\mathrm{k}})$ and $\nu(\omega_{\mathrm{k}},\hat{u}_{\max})$ as in (15) and $\boldsymbol{F}$, $\boldsymbol{f}$ and ϕ as in (21). To obtain the optimal (maximizing) reference current vector as in (39), the following necessary and sufficient conditions must be evaluated.

1) Necessary condition for a maximum: To find a maximum, the following *necessary* condition must be satisfied: The gradient[4] of the Lagrangian must be equal to the zero vector, i.e.

$$\boldsymbol{g}_{\mathfrak{L}}(\boldsymbol{i}_{\mathrm{s}}^k,\lambda):=\begin{pmatrix}\frac{\mathrm{d}\mathfrak{L}(\boldsymbol{i}_{\mathrm{s}}^k,\lambda)}{\mathrm{d}(\boldsymbol{i}_{\mathrm{s}}^k,\lambda)}\end{pmatrix}^{\top}=\begin{pmatrix}\left(\frac{\mathrm{d}\mathfrak{L}(\boldsymbol{i}_{\mathrm{s}}^k,\lambda)}{\mathrm{d}\boldsymbol{i}_{\mathrm{s}}^k}\right)^{\top}\\ \frac{\mathrm{d}\mathfrak{L}(\boldsymbol{i}_{\mathrm{s}}^k,\lambda)}{\mathrm{d}\lambda}\end{pmatrix}\overset{!}{=}\boldsymbol{0}_3\qquad\overset{(39)}{\Longrightarrow}\qquad\begin{pmatrix}-2\boldsymbol{A}\boldsymbol{i}_{\mathrm{s}}^k-2\boldsymbol{a}+\lambda(2\boldsymbol{B}\boldsymbol{i}_{\mathrm{s}}^k+2\boldsymbol{b})\\ (\boldsymbol{i}_{\mathrm{s}}^k)^{\top}\boldsymbol{B}\boldsymbol{i}_{\mathrm{s}}^k+2\boldsymbol{b}^{\top}\boldsymbol{i}_{\mathrm{s}}^k+\beta\end{pmatrix}\overset{!}{=}\boldsymbol{0}_3. \tag{41}$$

By defining

$$\boldsymbol{M}(\lambda):=\lambda\,\boldsymbol{B}-\boldsymbol{A}=\begin{bmatrix}\lambda\,b_{11}-a_{11} & \lambda\,b_{12}-a_{12}\\ \lambda\,b_{12}-a_{12} & \lambda\,b_{22}-a_{22}\end{bmatrix}\qquad\text{and}\qquad\boldsymbol{m}(\lambda):=\lambda\,\boldsymbol{b}-\boldsymbol{a}=\begin{pmatrix}\lambda\,b_1-a_1\\ \lambda\,b_2-a_2\end{pmatrix}, \tag{42}$$

one may rewrite the first two rows in (41) in the compact form

$$2\big[\lambda\,\boldsymbol{B}-\boldsymbol{A}\big]\boldsymbol{i}_{\mathrm{s}}^k+\big(\lambda\,\boldsymbol{b}-\boldsymbol{a}\big)\overset{(42)}{=}2\boldsymbol{M}(\lambda)\boldsymbol{i}_{\mathrm{s}}^k+2\boldsymbol{m}(\lambda)=\boldsymbol{0}_2 \tag{43}$$

and solving for $\boldsymbol{i}_{\mathrm{s}}^k=\boldsymbol{i}_{\mathrm{s}}^{k,\star}$ yields

$$\boldsymbol{i}_{\mathrm{s}}^{k,\star}(\lambda)=-\big[\lambda\,\boldsymbol{B}-\boldsymbol{A}\big]^{-1}\big(\lambda\,\boldsymbol{b}-\boldsymbol{a}\big)\overset{(42)}{=}-\boldsymbol{M}(\lambda)^{-1}\boldsymbol{m}(\lambda) \tag{44}$$

where

$$\boldsymbol{M}(\lambda)^{-1}=\big[\lambda\,\boldsymbol{B}-\boldsymbol{A}\big]^{-1}=\frac{1}{\det\boldsymbol{M}(\lambda)}\begin{bmatrix}\lambda\,b_{22}-a_{22} & -\lambda\,b_{12}+a_{12}\\ -\lambda\,b_{12}+a_{12} & \lambda\,b_{11}-a_{11}\end{bmatrix}=\big(\big[\lambda\,\boldsymbol{B}-\boldsymbol{A}\big]^{-1}\big)^{\top}=\big(\boldsymbol{M}(\lambda)^{-1}\big)^{\top}$$

and

$$\det\boldsymbol{M}(\lambda)=(\lambda\,b_{11}-a_{11})(\lambda\,b_{22}-a_{22})-(\lambda\,b_{12}-a_{12})^2=\big(\det\boldsymbol{B}\big)\lambda^2+\big(\det\big(\boldsymbol{B}-\boldsymbol{A}\big)-\det\boldsymbol{A}-\det\boldsymbol{B}\big)\lambda+\det\boldsymbol{A}.$$

[4]Note that, for some vectors $\boldsymbol{x},\boldsymbol{c}\in\mathbb{R}^n$ and a symmetric matrix $\boldsymbol{M}=\boldsymbol{M}^{\top}\in\mathbb{R}^{n\times n}$, the following hold $(\frac{\mathrm{d}\boldsymbol{c}^{\top}\boldsymbol{x}}{\mathrm{d}\boldsymbol{x}})^{\top}=(\frac{\mathrm{d}\boldsymbol{c}^{\top}\boldsymbol{x}}{\mathrm{d}x_1},\ldots,\frac{\mathrm{d}\boldsymbol{c}^{\top}\boldsymbol{x}}{\mathrm{d}x_n})^{\top}=(c_1,\ldots,c_n)^{\top}=\boldsymbol{c}$ and $(\frac{\mathrm{d}\boldsymbol{x}^{\top}\boldsymbol{M}\boldsymbol{x}}{\mathrm{d}\boldsymbol{x}})^{\top}=(\frac{\mathrm{d}\boldsymbol{x}^{\top}\boldsymbol{M}\boldsymbol{x}}{\mathrm{d}x_1},\ldots,\frac{\mathrm{d}\boldsymbol{x}^{\top}\boldsymbol{M}\boldsymbol{x}}{\mathrm{d}x_n})^{\top}=(\boldsymbol{M}+\boldsymbol{M}^{\top})\boldsymbol{x}=2\boldsymbol{M}\boldsymbol{x}$ (see [44, Proposition 10.7.1 i)]).

Inserting $\boldsymbol{i}_{\mathrm{s}}^k = \boldsymbol{i}_{\mathrm{s}}^{k,\star}(\lambda)$ as in (44) into the constraint quadric $Q_B(\boldsymbol{i}_{\mathrm{s}}^k)$ as in (39) gives a quartic polynomial in λ as follows

$$\left.\begin{array}{rcl} \boldsymbol{m}(\lambda)^\top \boldsymbol{M}(\lambda)^{-1}\boldsymbol{B}\,\boldsymbol{M}(\lambda)^{-1}\boldsymbol{m}(\lambda) - 2\boldsymbol{b}^\top \boldsymbol{M}(\lambda)^{-1}\boldsymbol{m}(\lambda) + \beta & = & 0 \quad \big| \quad \cdot \det\big(\boldsymbol{M}(\lambda)\big)^2 \\ \implies \qquad \chi_4(\lambda) := c_4\lambda^4 + c_3\lambda^3 + c_2\lambda^2 + c_1\lambda + c_0 & & \end{array}\right\} \tag{45}$$

with *real* coefficients

$$\left.\begin{array}{rcl} c_4 & := & -\big(b_{11}b_{22} - b_{12}^2\big)\big(b_{22}b_1^2 - 2b_1b_2b_{12} + b_{11}b_2^2 + \beta b_{12}^2 - b_{11}b_{22}\beta\big) \\ c_3 & := & 2(a_{11}b_{22} - 2a_{12}b_{12} + a_{22}b_{11})(b_{22}b_1^2 - 2b_1b_2b_{12} + b_{11}b_2^2 + \beta b_{12}^2 - b_{11}b_{22}\beta) \\ c_2 & := & a_1^2b_{11}b_{22}^2 - a_1^2b_{12}^2b_{22} - 2a_1a_2b_{11}b_{12}b_{22} + 2a_1a_2b_{12}^3 - 2a_1a_{11}b_1b_{22}^2 \\ & & +2a_1a_{11}b_2b_{12}b_{22} + 4a_1a_{12}b_1b_{12}b_{22} - 2a_1a_{12}b_2b_{11}b_{22} - 2a_1a_{12}b_2b_{12}^2 \\ & & -2a_1a_{22}b_1b_{12}^2 + 2a_1a_{22}b_2b_{11}b_{12} + a_2^2b_{11}^2b_{22} - a_2^2b_{11}b_{12}^2 + 2a_2a_{11}b_1b_{12}b_{22} \\ & & -2a_2a_{11}b_2b_{12}^2 - 2a_2a_{12}b_1b_{11}b_{22} - 2a_2a_{12}b_1b_{12}^2 + 4a_2a_{12}b_2b_{11}b_{12} \\ & & +2a_2a_{22}b_1b_{11}b_{12} - 2a_2a_{22}b_2b_{11}^2 - a_{11}^2b_2^2b_{22} + \beta a_{11}^2b_{22}^2 + 2a_{11}a_{12}b_1b_2b_{22} \\ & & +2a_{11}a_{12}b_2^2b_{12} - 4\beta a_{11}a_{12}b_{12}b_{22} - 4a_{11}a_{22}b_1^2b_{22} + 6a_{11}a_{22}b_1b_2b_{12} \\ & & -4a_{11}a_{22}b_2^2b_{11} + 4\beta a_{11}a_{22}b_{11}b_{22} - 2\beta a_{11}a_{22}b_{12}^2 + 3a_{12}^2b_1^2b_{22} - 10a_{12}^2b_1b_2b_{12} \\ & & +3a_{12}^2b_2^2b_{11} - 2\beta a_{12}^2b_{11}b_{22} + 6\beta a_{12}^2b_{12}^2 + 2a_{12}a_{22}b_1^2b_{12} + 2a_{12}a_{22}b_1b_2b_{11} \\ & & -4\beta a_{12}a_{22}b_{11}b_{12} - a_{22}^2b_1^2b_{11} + \beta a_{22}^2b_{11}^2 \\ c_1 & := & 2a_1^2a_{22}b_{12}^2 - 2b_{11}b_{22}a_1^2a_{22} - 4a_1a_2a_{12}b_{12}^2 + 4b_{11}b_{22}a_1a_2a_{12} + 4b_{22}a_1a_{11}a_{22}b_1 \\ & & -4a_1a_{11}a_{22}b_2b_{12} - 4b_{22}a_1a_{12}^2b_1 + 4a_1a_{12}^2b_2b_{12} + 2a_2^2a_{11}b_{12}^2 - 2b_{11}b_{22}a_2^2a_{11} \\ & & -4a_2a_{11}a_{22}b_1b_{12} + 4b_{11}a_2a_{11}a_{22}b_2 + 4a_2a_{12}^2b_1b_{12} - 4b_{11}a_2a_{12}^2b_2 + 2a_{11}^2a_{22}b_2^2 \\ & & -2b_{22}\beta a_{11}^2a_{22} - 2a_{11}a_{12}^2b_2^2 + 2b_{22}\beta a_{11}a_{12}^2 - 4a_{11}a_{12}a_{22}b_1b_2 + 4\beta a_{11}a_{12}a_{22}b_{12} \\ & & +2a_{11}a_{22}^2b_1^2 - 2b_{11}\beta a_{11}a_{22}^2 + 4a_{12}^3b_1b_2 - 4\beta a_{12}^3b_{12} - 2a_{12}^2a_{22}b_1^2 + 2b_{11}\beta a_{12}^2a_{22} \\ c_0 & := & b_{22}a_1^2a_{12}^2 - 2b_{12}a_1^2a_{12}a_{22} + b_{11}a_1^2a_{22}^2 - 2b_{22}a_1a_2a_{11}a_{12} + 2b_{12}a_1a_2a_{11}a_{22} + 2b_{12}a_1a_2a_{12}^2 \\ & & -2b_{11}a_1a_2a_{12}a_{22} + 2b_2a_1a_{11}a_{12}a_{22} - 2b_1a_1a_{11}a_{22}^2 - 2b_2a_1a_{12}^3 + 2b_1a_1a_{12}^2a_{22} + b_{22}a_2^2a_{11}^2 \\ & & -2b_{12}a_2^2a_{11}a_{12} + b_{11}a_2^2a_{12}^2 - 2b_2a_2a_{11}^2a_{22} + 2b_2a_2a_{11}a_{12}^2 + 2b_1a_2a_{11}a_{12}a_{22} - 2b_1a_2a_{12}^3 \\ & & +\beta a_{11}^2a_{22}^2 - 2\beta a_{11}a_{12}^2a_{22} + \beta a_{12}^4. \end{array}\right\} \tag{46}$$

2) Sufficient condition for a maximum: To obtain a *maximum* under an equality constraint, the Hessian of the Lagrangian $\mathfrak{L}(\boldsymbol{i}_{\mathrm{s}}^k, \lambda)$ must be *negative definite*, i.e.

$$\boldsymbol{H}_{\mathfrak{L}}(\boldsymbol{i}_{\mathrm{s}}^k, \lambda) := \tfrac{\mathrm{d}}{\mathrm{d}(\boldsymbol{i}_{\mathrm{s}}^k, \lambda)} \left(\tfrac{\mathrm{d}\,\mathfrak{L}(\boldsymbol{i}_{\mathrm{s}}^k, \lambda)}{\mathrm{d}(\boldsymbol{i}_{\mathrm{s}}^k, \lambda)}\right)^\top \overset{!}{<} 0. \tag{47}$$

The Hessian matrix is symmetric and given by

$$\boldsymbol{H}_{\mathfrak{L}}(\boldsymbol{i}_{\mathrm{s}}^k, \lambda) := \tfrac{\mathrm{d}}{\mathrm{d}(\boldsymbol{i}_{\mathrm{s}}^k, \lambda)} \left(\tfrac{\mathrm{d}\,\mathfrak{L}(\boldsymbol{i}_{\mathrm{s}}^k, \lambda)}{\mathrm{d}(\boldsymbol{i}_{\mathrm{s}}^k, \lambda)}\right)^\top = \begin{bmatrix} 2\boldsymbol{M}(\lambda) & 2\boldsymbol{B}\boldsymbol{i}_{\mathrm{s}}^k + 2\boldsymbol{b} \\ (2\boldsymbol{B}\boldsymbol{i}_{\mathrm{s}}^k + 2\boldsymbol{b})^\top & 0 \end{bmatrix} = \boldsymbol{H}_{\mathfrak{L}}(\boldsymbol{i}_{\mathrm{s}}^k, \lambda)^\top \in \mathbb{R}^{3\times 3}. \tag{48}$$

The Hessian $\boldsymbol{H}_{\mathfrak{L}}(\boldsymbol{i}_{\mathrm{s}}^k, \lambda)$ is negative definite if and only if all its leading principal minors[5] have alternating signs (see [44, Prop. 8.2.8] in combination with [44, Prop. 2.7.1][6]). More precisely, first and third leading principle minor of (48) must be *negative* whereas the second leading principle minor must be *positive*, i.e. $2m_{11}(\lambda^\star) \overset{(42)}{=} 2\big(a_{11} + \lambda^\star b_{11}\big) < 0$ (first leading principal minor), $\det\big(2\boldsymbol{M}(\lambda^\star)\big) = 2^2 \det \boldsymbol{M}(\lambda^\star) > 0$ (second leading principal minor) and $\det\big(\boldsymbol{H}_{\mathfrak{L}}(\boldsymbol{i}_{\mathrm{s}}^k, \lambda^\star)\big) < 0$ (third leading principal minor). Hence, the optimal (real) Lagrangian multiplier $\lambda^\star \in \mathbb{R}$ must satisfy

$$\left.\begin{array}{rcl} \text{(i)} \quad \lambda^\star < -\dfrac{a_{11}}{b_{11}} & \implies & 2\big(a_{11} + \lambda^\star b_{11}\big) < 0 \\ \text{(ii)} \quad \lambda^\star > \dfrac{\big(\det\big(\boldsymbol{B}-\boldsymbol{A}\big) - \det\boldsymbol{A} - \det\boldsymbol{B}\big)}{-\operatorname{sign}(\det\boldsymbol{B})\det\boldsymbol{B}}\left(1 \pm \sqrt{1 - \dfrac{4\det\boldsymbol{A}\det\boldsymbol{B}}{\big(\det\big(\boldsymbol{B}-\boldsymbol{A}\big) - \det\boldsymbol{A} - \det\boldsymbol{B}\big)^2}}\right) & \implies & \det\boldsymbol{M}(\lambda^\star) > 0. \end{array}\right\} \tag{49}$$

Clearly, the conditions (i) and (ii) in (49) must be satisfied simultaneously and, therefore, imply negative definiteness of $\boldsymbol{M}(\lambda^\star) = \lambda^\star\boldsymbol{B} - \boldsymbol{A}$. Moreover, by defining

$$\boldsymbol{C}(\boldsymbol{i}_{\mathrm{s}}^k, \lambda^\star) := \begin{bmatrix} \boldsymbol{I}_2, & \boldsymbol{M}(\lambda^\star)^{-1}(\boldsymbol{B}\boldsymbol{i}_{\mathrm{s}}^k + \boldsymbol{b}) \\ \boldsymbol{0}_2^\top, & 1 \end{bmatrix} \in \mathbb{R}^{3\times 3} \quad \text{with} \quad \det\boldsymbol{C}(\boldsymbol{i}_{\mathrm{s}}^k, \lambda^\star) = \det\boldsymbol{C}(\boldsymbol{i}_{\mathrm{s}}^k, \lambda^\star)^\top = 1$$

and by invoking [44, Fact 2.16.2], the Hessian matrix

$$\boldsymbol{H}_{\mathfrak{L}}(\boldsymbol{i}_{\mathrm{s}}^k, \lambda^\star) = 2\boldsymbol{C}(\boldsymbol{i}_{\mathrm{s}}^k, \lambda^\star)^\top \begin{bmatrix} \boldsymbol{M}(\lambda^\star), & \boldsymbol{0}_2 \\ \boldsymbol{0}_2^\top, & -\big((\boldsymbol{i}_{\mathrm{s}}^k)^\top\boldsymbol{B}^\top + \boldsymbol{b}^\top\big)\boldsymbol{M}(\lambda^\star)^{-1}\big(\boldsymbol{B}\boldsymbol{i}_{\mathrm{s}}^k + \boldsymbol{b}\big) \end{bmatrix} \boldsymbol{C}(\boldsymbol{i}_{\mathrm{s}}^k, \lambda^\star)$$

[5]The i-th leading principle minor is the determinant of the (i,i)-north-western submatrix of the matrix [44, Prop. 8.2.7].

[6]I.e., for all $\gamma \in \mathbb{R}$ and $\boldsymbol{A} \in \mathbb{R}^{n\times n}$, the following holds $\det(\gamma\boldsymbol{A}) = (\gamma)^n \det(\boldsymbol{A})$. Hence, application of the Sylvester's criterion to negative definite matrices yields alternating signs of the leading principle minors.

can be written as product of three matrices. Hence,

$$\det\big[\boldsymbol{H}_{\mathfrak{L}}(\boldsymbol{i}_{\mathrm{s}}^k,\lambda^\star)\big] = -2\underbrace{\big((\boldsymbol{i}_{\mathrm{s}}^k)^\top\boldsymbol{B}^\top+\boldsymbol{b}^\top\big)\boldsymbol{M}(\lambda^\star)^{-1}\big(\boldsymbol{B}\boldsymbol{i}_{\mathrm{s}}^k+\boldsymbol{b}\big)}_{=:\ \gamma\in\mathbb{R}}\cdot\det\boldsymbol{M}(\lambda^\star),$$

which, with $\det\boldsymbol{C}(\boldsymbol{i}_{\mathrm{s}}^k,\lambda^\star)=\det\boldsymbol{C}(\boldsymbol{i}_{\mathrm{s}}^k,\lambda^\star)^\top=1$ and negative definiteness of $\boldsymbol{M}(\lambda^\star)=\big[\boldsymbol{A}+\lambda^\star\boldsymbol{B}\big]\overset{(49)}{<}0$, implies that $\gamma=\|\boldsymbol{B}\boldsymbol{i}_{\mathrm{s}}^k+\boldsymbol{b}\|^2_{\boldsymbol{M}(\lambda^\star)}<0$ (a weighted norm with negative definite $\boldsymbol{M}(\lambda^\star)<0$) is negative for all *non-zero* vectors

$$\begin{aligned}\boldsymbol{B}\boldsymbol{i}_{\mathrm{s}}^{k,\star}(\lambda^\star)+\boldsymbol{b} &\overset{(44)}{=} -\lambda^\star\boldsymbol{B}\big[\boldsymbol{A}+\lambda^\star\boldsymbol{B}\big]^{-1}\boldsymbol{b}+\boldsymbol{b}=-\big(-\boldsymbol{I}_2+\lambda^\star\boldsymbol{B}\big[\boldsymbol{A}+\lambda^\star\boldsymbol{B}\big]^{-1}\big)\boldsymbol{b}\\ &\overset{\text{[44, Cor. 2.8.10]}}{=} \big[\boldsymbol{A}+\lambda^\star\boldsymbol{B}\big]^{-1}\boldsymbol{b}\overset{(49)}{\neq}\boldsymbol{0}_2\quad\text{for all}\quad\lambda^\star\text{ as in (49).}\end{aligned}$$

Concluding, for the optimal $\lambda^\star$, the third leading principle minor is (always) negative, i.e. $\det\big[\boldsymbol{H}_{\mathfrak{L}}(\boldsymbol{i}_{\mathrm{s}}^k,\lambda^\star)\big]<0$. By checking definiteness of (47) for $\lambda^\star\in\{\lambda_1^\star,\ldots,\lambda_4^\star\}$ where $\boldsymbol{M}(\lambda^\star)>0$, the analytical solution for the optimal reference current vector is finally given by

$$\boxed{\boldsymbol{i}_{\mathrm{s,ref}}^k\overset{(39)}{:=}\boldsymbol{i}_{\mathrm{s}}^{k,\star}(\lambda^\star)\overset{(44)}{=}-\boldsymbol{M}(\lambda^\star)^{-1}\boldsymbol{m}(\lambda^\star)=-\big[\lambda^\star\boldsymbol{B}-\boldsymbol{A}\big]^{-1}\big(\lambda^\star\boldsymbol{b}-\boldsymbol{a}\big).}\tag{50}$$

Remark A.1 (The case $\boldsymbol{m}(\lambda)=\boldsymbol{0}_2$ for all $\lambda\in\mathbb{C}$)**.** *Note that the optimal reference current vector* (50) *only gives a non-trivial solution if $\boldsymbol{m}(\lambda)=\lambda\boldsymbol{b}-\boldsymbol{a}\neq 0$. This is not true for RSMs, where $\psi_{\mathrm{pm}}=0$ and, hence, $\boldsymbol{t}\overset{(9)}{=}\boldsymbol{0}_2$, $\boldsymbol{v}(\omega_{\mathrm{k}})\overset{(15)}{=}\boldsymbol{0}_2$ and $\boldsymbol{f}\overset{(21)}{=}\boldsymbol{0}_2$. To solve these optimization problems,* (39) *must be re-formulated by shifting/translating the quadrics $Q_A(\boldsymbol{i}_{\mathrm{s}}^k)$ and $Q_B(\boldsymbol{i}_{\mathrm{s}}^k)$ by some non-zero but constant $\boldsymbol{x}_{\mathrm{s}}\in\mathbb{R}^2$. The shifted quadrics $Q_A(\bar{\boldsymbol{i}}_{\mathrm{s}}^k+\boldsymbol{x}_{\mathrm{s}})$ and $Q_B(\bar{\boldsymbol{i}}_{\mathrm{s}}^k+\boldsymbol{x}_{\mathrm{s}})$ are obtained by inserting $\boldsymbol{i}_{\mathrm{s}}^k=\bar{\boldsymbol{i}}_{\mathrm{s}}^k+\boldsymbol{x}_{\mathrm{s}}$ into* (39) *(for more details see Appendix D).*

Remark A.2 (Normalization)**.** *For a numerical implementation, a normalization of* (8) *might be beneficial yielding a less ill-conditioned optimization problem (the coefficients of the fourth-order polynomials heavily differ in magnitude). The normalized version of* (8) *is*

$$\bar{\boldsymbol{u}}_{\mathrm{s}}^k=\bar{R}_{\mathrm{s}}\bar{\boldsymbol{i}}_{\mathrm{s}}^k+\bar{\omega}_{\mathrm{k}}\boldsymbol{J}\bar{\boldsymbol{L}}_{\mathrm{s}}^k\bar{\boldsymbol{i}}_{\mathrm{s}}^k+\bar{\omega}_{\mathrm{k}}\boldsymbol{J}\bar{\boldsymbol{\psi}}_{\mathrm{pm}}^k\tag{51}$$

where the normalized (unitless) quantities and parameters are defined by

$$\bar{\boldsymbol{u}}_{\mathrm{s}}^k:=\frac{\boldsymbol{u}_{\mathrm{s}}^k}{\hat{u}_{\max}},\quad\bar{R}_{\mathrm{s}}:=\frac{R_{\mathrm{s}}}{\hat{u}_{\max}/\hat{\imath}_{\max}},\quad\bar{\boldsymbol{i}}_{\mathrm{s}}^k:=\frac{\boldsymbol{i}_{\mathrm{s}}^k}{\hat{\imath}_{\max}},\quad\bar{\omega}_{\mathrm{k}}:=\frac{\omega_{\mathrm{k}}}{\omega_{\mathrm{k,nom}}},\quad\bar{\boldsymbol{L}}_{\mathrm{s}}^k:=\frac{\omega_{\mathrm{k,nom}}}{\hat{u}_{\max}/\hat{\imath}_{\max}}\boldsymbol{L}_{\mathrm{s}}^k\ \text{ and }\ \bar{\boldsymbol{\psi}}_{\mathrm{pm}}^k:=\frac{\omega_{\mathrm{k,nom}}}{\hat{u}_{\max}}\boldsymbol{\psi}_{\mathrm{pm}}^k.$$

The normalized (unitless) machine torque and its reference are as follows

$$\bar{m}_{\mathrm{m}}:=\frac{\omega_{\mathrm{k,nom}}}{\hat{u}_{\max}\hat{\imath}_{\max}}m_{\mathrm{m}}\qquad\text{and}\qquad\bar{m}_{\mathrm{m,ref}}:=\frac{\omega_{\mathrm{k,nom}}}{\hat{u}_{\max}\hat{\imath}_{\max}}m_{\mathrm{m,ref}}.$$

3) Analytical computation of the roots of a quartic polynomial: The discriminant of the quartic polynomial $\chi_4(\lambda)$ as in (45) can be computed as follows

$$\begin{aligned}\Delta:=\;&256c_4^3c_0^3-192c_4^2c_3c_1c_0^2-128c_4^2c_2^2c_0^2+144c_4^2c_2c_1^2c_0-27c_4^2c_1^4\\&+144c_4c_3^2c_2c_0^2-6c_4c_3^2c_1^2c_0-80c_4c_3c_2^2c_1c_0+18c_4c_3c_2c_1^3+16c_4c_2^4c_0\\&-4c_4c_2^3c_1^2-27c_3^4c_0^2+18c_3^3c_2c_1c_0-4c_3^3c_1^3-4c_3^2c_2^3c_0+c_3^2c_2^2c_1^2.\end{aligned}\tag{52}$$

For $\Delta<0$, the quartic polynomial (45) has two real and two complex roots (all distinct); for $\Delta>0$, (45) has four real or four complex roots (all distinct) and, for $\Delta=0$, (45) has at least two equal roots (for more details see [41]). Euler's solution will be presented (for details see [45]) which is based on the *depressed* (and monic) quartic polynomial given by

$$\chi_{4,\mathrm{dep}}(y):=y^4+py^2+qy+r\tag{53}$$

with real coefficients

$$p:=\tfrac{1}{c_4^2}\Big(c_2\,c_4-\tfrac{3\,c_3^2}{8}\Big),\quad q:=\tfrac{1}{c_4^3}\Big(\tfrac{c_3^3}{8}-\tfrac{c_2\,c_3\,c_4}{2}+c_1\,c_4^2\Big)\quad\text{and}\quad r:=\tfrac{1}{c_4^4}\Big(-\tfrac{3c_3^4}{256}+c_4^3c_0-\tfrac{c_4^2c_3c_2}{4}+\tfrac{c_4c_3^2c_2}{16}\Big).\tag{54}$$

The depressed quartic polynomial (53) is obtained by inserting $\lambda:=y-\frac{c_3}{4c_4}$ into (45). To compute the roots of the depressed quartic, one needs to find the three roots $z_1^\star$, $z_2^\star$ and $z_3^\star$ of Euler's resolvent cubic polynomial given by

$$\chi_{3,\mathrm{res}}(z):=z^3+2pz^2+(p^2-4r)\,z-q^2,\tag{55}$$

where p, q and r are as in (54). In Appendix A4, the analytical solution to compute the three roots $z_1^\star$, $z_2^\star$ and $z_3^\star$ of the resolvent cubic (55) is presented. Finally, for known resolvent roots $z_1^\star$, $z_2^\star$ and $z_3^\star$, the four roots $\lambda_1^\star$, $\lambda_2^\star$, $\lambda_3^\star$ and $\lambda_4^\star$ of the

quartic polynomial (45) are given by

$$\left.\begin{array}{rcll} \lambda_1^\star &=& \frac{(-1)^l}{2}\Big(\quad \sqrt{z_1^\star} + \sqrt{z_2^\star} + \sqrt{z_3^\star}\Big) - \frac{c_3}{4c_4}, & \\ \lambda_2^\star &=& \frac{(-1)^l}{2}\Big(\quad \sqrt{z_1^\star} - \sqrt{z_2^\star} - \sqrt{z_3^\star}\Big) - \frac{c_3}{4c_4}, & \\ \lambda_3^\star &=& \frac{(-1)^l}{2}\Big(-\sqrt{z_1} + \sqrt{z_2^\star} - \sqrt{z_3^\star}\Big) - \frac{c_3}{4c_4}, & \text{and} \\ \lambda_4^\star &=& \frac{(-1)^l}{2}\Big(-\sqrt{z_1} - \sqrt{z_2^\star} + \sqrt{z_2^\star}\Big) - \frac{c_3}{4c_4}, & \end{array}\right\} \tag{56}$$

where $l \in \{0, 1\}$ must be chosen such that [45]

$$(-1)^l\big(\lambda_1^\star\lambda_2^\star\lambda_3^\star + \lambda_1^\star\lambda_2^\star\lambda_4^\star + \lambda_1^\star\lambda_3^\star\lambda_4^\star + \lambda_2^\star\lambda_3^\star\lambda_4^\star\big) = -q.$$

4) Analytical computation of the roots of a cubic polynomial: Consider the monic cubic polynomial with real coefficients given by

$$\chi_3(z) := z^3 + d_2z^2 + d_1z + d_0 \qquad \text{where} \qquad d_2, \ldots, d_0 \in \mathbb{R}. \tag{57}$$

Its roots $z_1^\star$, $z_2^\star$ and $z_3^\star$ can be computed analytically as follows [46, p. 17]. Note that the cubic polynomial $\chi_3(z)$ has (a) one real and a pair of complex conjugate roots if $\tilde{q}^3 + \tilde{r}^2 > 0$, (b) only real roots but at least two are equal if $\tilde{q}^3 + \tilde{r}^2 = 0$, and (c) only real roots but all are distinct if $\tilde{q}^3 + \tilde{r}^2 < 0$. For the following, define

$$\tilde{q} := \frac{d_1}{3} - \frac{d_2^2}{9} \qquad \text{and} \qquad \tilde{r} := \frac{d_1d_2 - 3d_0}{6} - \frac{d_2^3}{27}.$$

Then, for

$$s_1 := \sqrt[3]{\tilde{r} + \sqrt{\tilde{q}^3 + \tilde{r}^2}} \qquad \text{and} \qquad s_2 := \sqrt[3]{\tilde{r} - \sqrt{\tilde{q}^3 + \tilde{r}^2}},$$

the three roots of the cubic polynomial (57) are given by

$$z_1^\star = (s_1 + s_2) - \tfrac{d_2}{3} \quad \text{and} \quad z_{2,3}^\star = -\tfrac{1}{2}(s_1 + s_2) - \tfrac{d_2}{3} \pm \jmath\tfrac{\sqrt{3}}{2}(s_1 - s_2). \tag{58}$$

B. Computation of the quadrics (implicit expressions) for MTPC, MTPV and MTPF

To derive the implicit forms presented in Sec. III-B, the first two rows of the gradient (41) must be set to zero, i.e.,

$$\boldsymbol{A}\boldsymbol{i}_{\mathrm{s}}^k + \boldsymbol{a} + \lambda(\boldsymbol{B}\boldsymbol{i}_{\mathrm{s}}^k + \boldsymbol{b}) = \boldsymbol{0}_2. \tag{59}$$

Rewriting this equation component wise, one may solve and eliminate for the Lagrangian multiplier λ as follows

$$\begin{aligned} \lambda &= -\frac{(a_{11},\, a_{12})\boldsymbol{i}_{\mathrm{s}}^k + a_1}{(b_{11},\, b_{12})\boldsymbol{i}_{\mathrm{s}}^k + b_1} = -\frac{(a_{12},\, a_{22})\boldsymbol{i}_{\mathrm{s}}^k + a_2}{(b_{12},\, b_{22})\boldsymbol{i}_{\mathrm{s}}^k + b_2} \\ \implies &\quad \big((a_{11},\, a_{12})\boldsymbol{i}_{\mathrm{s}}^k + a_1\big)\big((b_{12},\, b_{22})\boldsymbol{i}_{\mathrm{s}}^k + b_2\big) - \big((a_{12},\, a_{22})\boldsymbol{i}_{\mathrm{s}}^k + a_2\big)\big((b_{11},\, b_{12})\boldsymbol{i}_{\mathrm{s}}^k + b_1\big) = 0. \end{aligned} \tag{60}$$

Re-arranging leads to the following quadric

$$(\boldsymbol{i}_{\mathrm{s}}^k)^\top \boldsymbol{M}_{\mathrm{X}}\boldsymbol{i}_{\mathrm{s}}^k + 2\boldsymbol{m}_{\mathrm{X}}^\top\boldsymbol{i}_{\mathrm{s}}^k + \mu_{\mathrm{X}}$$

where

$$\left.\begin{array}{rcl} \boldsymbol{M}_{\mathrm{X}} = \boldsymbol{M}_{\mathrm{X}}^\top &:=& \begin{bmatrix} a_{11}b_{12} - a_{12}b_{11} & \frac{1}{2}\big(a_{11}b_{22} + a_{12}b_{12} - a_{22}b_{11} - a_{12}b_{12}\big) \\ \frac{1}{2}\big(a_{11}b_{22} + a_{12}b_{12} - a_{22}b_{11} - a_{12}b_{12}\big) & a_{12}b_{22} - a_{22}b_{12} \end{bmatrix} \\ &\overset{(38)}{=}& \begin{bmatrix} a_{11}b_{12} - a_{12}b_{11} & \frac{1}{2}\big(a_{11}b_{22} - a_{22}b_{11}\big) \\ \frac{1}{2}\big(a_{11}b_{22} - a_{22}b_{11}\big) & a_{12}b_{22} - a_{22}b_{12} \end{bmatrix}, \\ \boldsymbol{m}_{\mathrm{X}} &:=& \frac{1}{2}\begin{pmatrix} a_{11}b_2 + a_1b_{12} - a_{12}b_1 - a_2b_{11} \\ a_{12}b_2 + a_1b_{22} - a_{22}b_1 - a_2b_{12} \end{pmatrix} \qquad \text{and} \\ \mu_{\mathrm{X}} &:=& a_1b_2 - a_2b_1. \end{array}\right\} \tag{61}$$

The corresponding matrix $\boldsymbol{M}_{\mathrm{X}}$, vector $\boldsymbol{m}_{\mathrm{X}}$ and scalar μ_{X} in (59) with $\mathrm{X} \in \{\mathrm{C}, \mathrm{V}, \mathrm{F}\}$ are obtained for

- the MTPC hyperbola (23) (i.e. $\mathrm{X} = \mathrm{C}$) by setting $\boldsymbol{A} = \boldsymbol{I}_2$, $\boldsymbol{a} = (0,\, 0)^\top$, $\boldsymbol{B} = \boldsymbol{T}$ and $\boldsymbol{b} = \boldsymbol{t}$;
- the MTPV hyperbola (29) (i.e. $\mathrm{X} = \mathrm{V}$) by setting $\boldsymbol{A} = \boldsymbol{V}(\omega_{\mathrm{k}})$, $\boldsymbol{a} = \boldsymbol{v}(\omega_{\mathrm{k}})$, $\boldsymbol{B} = \boldsymbol{T}$ and $\boldsymbol{b} = \boldsymbol{t}$; and
- the MTPF hyperbola (33) (i.e. $\mathrm{X} = \mathrm{F}$) by setting $\boldsymbol{A} = \boldsymbol{F}$, $\boldsymbol{a} = \boldsymbol{f}$, $\boldsymbol{B} = \boldsymbol{T}$ and $\boldsymbol{b} = \boldsymbol{t}$,

with $\boldsymbol{T}$ and $\boldsymbol{t}$ as in (9), $\boldsymbol{V}(\omega_{\mathrm{k}})$ and $\boldsymbol{v}(\omega_{\mathrm{k}})$ as in (15) and $\boldsymbol{F}$ and $\boldsymbol{f}$ as in (21), respectively.

C. Explicit expressions for current circle, voltage ellipse, and torque, MTPC, MTPV and MTPF hyperbolas

Consider an arbitrary quadric $Q_A(\boldsymbol{i}_{\mathrm{s}}^k)$ as in (37) where $\boldsymbol{A}$, $\boldsymbol{a}$ (and there respective entries a_{ij} and a_i) and α are as in (38). An explicit expression for $Q_A(\boldsymbol{i}_{\mathrm{s}}^k)$ can be obtained by solving $Q_A(\boldsymbol{i}_{\mathrm{s}}^k)$ as in (37) for the quadrature current i_{s}^q. To derive an explicit expression, different cases must be taken into account (like signs or whether certain parameters are zero or not) which makes the use of explicit expressions tedious. Assuming the explicit expression of the quadric $Q_A(\boldsymbol{i}_{\mathrm{s}}^k)$ as in (37) exists, it is given by

$$\mathbb{A}(i_{\mathrm{s}}^d) = -\frac{a_{12}i_{\mathrm{s}}^d + a_2}{a_{22}} \pm \frac{\sqrt{\big(a_{12}i_{\mathrm{s}}^d + a_2\big)^2 - a_{22}\big(a_{11}(i_{\mathrm{s}}^d)^2 + 2a_1 i_{\mathrm{s}}^d + \alpha\big)}}{a_{22}}. \tag{62}$$

Clearly, to have a meaningful expression, the following must hold: $a_{22} \neq 0$ and $\big(a_{12}i_{\mathrm{s}}^d + a_2\big)^2 - a_{22}\big(a_{11}(i_{\mathrm{s}}^d)^2 + 2a_1 i_{\mathrm{s}}^d + \alpha\big) \geq 0$ for all $i_{\mathrm{s}}^d \in \mathbb{R}$ (which might not hold in general; leading to different cases where (62) will hold). To compute the explicit expressions for torque, current circle, voltage ellipse, MTPC, MTPF and MTPV hyperbola, the corresponding matrix $\boldsymbol{A}$, vector $\boldsymbol{a}$ and scalar α must be chosen properly (e.g. for the voltage ellipse (17), choose $\boldsymbol{A} = \boldsymbol{V}(\omega_{\mathrm{k}})$, $\boldsymbol{a} = \boldsymbol{v}(\omega_{\mathrm{k}})$ and $\alpha = \nu(\omega_{\mathrm{k}}, \hat{u}_{\max})$ with $\boldsymbol{V}(\omega_{\mathrm{k}})$, $\boldsymbol{v}(\omega_{\mathrm{k}})$ and $\nu(\omega_{\mathrm{k}}, \hat{u}_{\max})$ as in (15)).

D. Computation of the intersection points of two arbitrary quadrics

To find the intersection point(s) $\boldsymbol{x}^\star$ of two arbitrary quadrics $Q_A(\boldsymbol{x})$ and $Q_B(\boldsymbol{x})$ as in (37), there are several possible algorithms. In this paper, an algorithm is presented which leads again to a problem of 'finding the roots of a fourth-order polynomial' and hence can be solved analytically. For the following, introduce

$$\boldsymbol{D} := \begin{bmatrix} d_{11} & d_{12} \\ d_{12} & d_{22} \end{bmatrix} \in \mathbb{R}^{2\times 2},\ \boldsymbol{d} := \begin{pmatrix} d_1 \\ d_2 \end{pmatrix} \in \mathbb{R}^2,\ \boldsymbol{x}_{\mathrm{s}} \in \mathbb{R}^2,\ \boldsymbol{M} := \begin{bmatrix} m_{11} & m_{12} \\ m_{12} & m_{22} \end{bmatrix} \in \mathbb{R}^{2\times 2}, \boldsymbol{m} := \begin{pmatrix} m_1 \\ m_2 \end{pmatrix} \in \mathbb{R}^2, \text{ and } \mu \in \mathbb{R}$$

and the quadric

$$Q_M(\boldsymbol{x}) := \boldsymbol{x}^\top \boldsymbol{M}\boldsymbol{x} + 2\boldsymbol{m}^\top \boldsymbol{x} + \mu \tag{63}$$

To compute the analytical solutions of the intersection points of the quadrics $Q_A(\boldsymbol{x})$ and $Q_B(\boldsymbol{x})$, three different cases must be considered:

(i) If $\alpha \neq 0$ and $\beta \neq 0$ in (37), then, for $\boldsymbol{D} := \left(\frac{\boldsymbol{A}}{\alpha} - \frac{\boldsymbol{B}}{\beta}\right)$ and $\boldsymbol{d} := \left(\frac{\boldsymbol{a}}{\alpha} - \frac{\boldsymbol{b}}{\beta}\right)$, define the difference quadric of the scaled quadrics as follows

$$Q_D(\boldsymbol{x}) := \boldsymbol{x}^\top \boldsymbol{D}\boldsymbol{x} + 2\boldsymbol{d}^\top \boldsymbol{x} = \boldsymbol{x}^\top \left(\tfrac{\boldsymbol{A}}{\alpha} - \tfrac{\boldsymbol{B}}{\beta}\right)\boldsymbol{x} + 2\left(\tfrac{\boldsymbol{a}}{\alpha} - \tfrac{\boldsymbol{b}}{\beta}\right)^\top \boldsymbol{x} = 0, \tag{64}$$

and set $\boldsymbol{M} := \boldsymbol{A}$, $\boldsymbol{m} := \boldsymbol{a}$ and $\mu := \alpha$ (or $\boldsymbol{M} := \boldsymbol{B}$, $\boldsymbol{m} := \boldsymbol{b}$ and $\mu := \beta$ in (63)). Both is possible and does not alter the result.

(ii) If $\alpha = 0$ and $\beta \neq 0$ in (37), then set $\boldsymbol{D} := \boldsymbol{A}$, $\boldsymbol{d} := \boldsymbol{a}$ in (64), and $\boldsymbol{M} := \boldsymbol{B}$, $\boldsymbol{m} := \boldsymbol{b}$ and $\mu := \beta$ in (63); *or* if $\alpha \neq 0$ and $\beta = 0$ in (37), then set $\boldsymbol{D} := \boldsymbol{B}$, $\boldsymbol{d} := \boldsymbol{b}$ in (64), and $\boldsymbol{M} := \boldsymbol{A}$, $\boldsymbol{m} := \boldsymbol{a}$ and $\mu := \alpha$ in (63).

(iii) If $\alpha = 0$ and $\beta = 0$ in (37), the quadrics $Q_A(\boldsymbol{x})$ and $Q_B(\boldsymbol{x})$ must be shifted (translated) by $\boldsymbol{x}_{\mathrm{s}} \in \mathbb{R}^2 \setminus \{\boldsymbol{0}_2\}$ by inserting $\boldsymbol{x} := \boldsymbol{y} + \boldsymbol{x}_{\mathrm{s}}$ into (37), i.e.

$$Q_A(\boldsymbol{y} + \boldsymbol{x}_{\mathrm{s}}) := \boldsymbol{y}^\top \boldsymbol{A}\boldsymbol{y} + 2\underbrace{(\boldsymbol{x}_{\mathrm{s}}^\top \boldsymbol{A} + \boldsymbol{a}^\top)}_{=:\,\boldsymbol{a}_{\mathrm{s}}^\top}\boldsymbol{y} + \underbrace{\boldsymbol{x}_{\mathrm{s}}^\top \boldsymbol{A}\boldsymbol{x}_{\mathrm{s}} + 2\boldsymbol{a}^\top \boldsymbol{x}_{\mathrm{s}}}_{\alpha_{\mathrm{s}}} \text{ and}$$

$$Q_B(\boldsymbol{y} + \boldsymbol{x}_{\mathrm{s}}) := \boldsymbol{y}^\top \boldsymbol{B}\boldsymbol{y} + 2\underbrace{(\boldsymbol{x}_{\mathrm{s}}^\top \boldsymbol{B} + \boldsymbol{b}^\top)}_{=:\,\boldsymbol{b}_{\mathrm{s}}^\top}\boldsymbol{y} + \underbrace{\boldsymbol{x}_{\mathrm{s}}^\top \boldsymbol{B}\boldsymbol{x}_{\mathrm{s}} + 2\boldsymbol{b}^\top \boldsymbol{x}_{\mathrm{s}}}_{\beta_{\mathrm{s}}},$$

such that the shifted scalars are non-zero, i.e. $\alpha_{\mathrm{s}} \neq 0$ and $\beta_{\mathrm{s}} \neq 0$. Then, case (i) holds true again (but now in $\boldsymbol{y}$) and one sets $\boldsymbol{D} := \left(\frac{\boldsymbol{A}}{\alpha_{\mathrm{s}}} - \frac{\boldsymbol{B}}{\beta_{\mathrm{s}}}\right)$, $\boldsymbol{d} := \left(\frac{\boldsymbol{a}_{\mathrm{s}}}{\alpha_{\mathrm{s}}} - \frac{\boldsymbol{b}_{\mathrm{s}}}{\beta_{\mathrm{s}}}\right)$ in (64), $\boldsymbol{M} := \boldsymbol{A}$, $\boldsymbol{m} := \boldsymbol{a}_{\mathrm{s}}$ and $\mu := \alpha_{\mathrm{s}}$ (or $\boldsymbol{M} := \boldsymbol{B}$, $\boldsymbol{m} := \boldsymbol{b}_{\mathrm{s}}$ and $\mu := \beta_{\mathrm{s}}$) in (63). Finally, to obtain the intersections points $\boldsymbol{x}^\star$, the solution $\boldsymbol{y}^\star$ must be translated again, i.e. $\boldsymbol{x}^\star = \boldsymbol{y}^\star + \boldsymbol{x}_{\mathrm{s}}$.

Note that, for all three cases (i), (ii) and (iii)[7], $\boldsymbol{D} = \boldsymbol{D}^\top$ and one may rewrite (64) as follows

$$Q_D(\boldsymbol{x}) = \boldsymbol{x}^\top \boldsymbol{D}\boldsymbol{x} + 2\boldsymbol{d}^\top \boldsymbol{x} = \boldsymbol{x}^\top \big(\underbrace{\boldsymbol{D}\boldsymbol{x} + 2\boldsymbol{d}}_{\stackrel{!}{=}\gamma \boldsymbol{J}\boldsymbol{x}}\big) = 0. \tag{65}$$

Since the vectors $\boldsymbol{J}\boldsymbol{x}$ (or $\boldsymbol{J}^\top \boldsymbol{x}$) and $\boldsymbol{x}$ are perpendicular to each other, the following holds $\gamma(\boldsymbol{J}\boldsymbol{x})^\top \boldsymbol{x} = \gamma \boldsymbol{x}^\top \boldsymbol{J}^\top \boldsymbol{x} = 0 = \gamma \boldsymbol{x}^\top \boldsymbol{J}\boldsymbol{x}$ for all $\gamma \in \mathbb{R} \setminus \{0\}$ and, so, (65) is clearly satisfied for $\boldsymbol{D}\boldsymbol{x} + 2\boldsymbol{d} \stackrel{!}{=} \gamma \boldsymbol{J}\boldsymbol{x}$ (the factor γ is necessary to allow for scaled versions of the vector $\boldsymbol{J}\boldsymbol{x}$; such that different lengths are admissible). Hence, one obtains

$$\big[\boldsymbol{D} - \gamma \boldsymbol{J}\big]\boldsymbol{x} + 2\boldsymbol{d} = \boldsymbol{0}_2 \implies \boxed{\boldsymbol{x}(\gamma) = -2\big[\boldsymbol{D} - \gamma \boldsymbol{J}\big]^{-1}\boldsymbol{d}} \text{ where } \big[\boldsymbol{D} - \gamma \boldsymbol{J}\big]^{-1} = \frac{1}{\gamma^2 + d_{11}d_{22} - d_{12}^2}\begin{bmatrix} d_{22}, & -d_{12} - \gamma \\ \gamma - d_{12}, & d_{11} \end{bmatrix}.$$

[7]For case (iii), substitute $\boldsymbol{y}$ for $\boldsymbol{x}$.

Inserting $\boldsymbol{x}(\gamma)$ as above into the quadric $Q_M(\boldsymbol{x})$ as in (63) gives a fourth-order polynomial in γ, i.e.

$$\left.\begin{array}{rcl} 4\boldsymbol{d}^\top(\big[\boldsymbol{D}-\gamma\boldsymbol{J}\big]^{-1})^\top\boldsymbol{M}\big[\boldsymbol{D}-\gamma\boldsymbol{J}\big]^{-1}\boldsymbol{d}-4\boldsymbol{m}^\top\big[\boldsymbol{D}-\gamma\boldsymbol{J}\big]^{-1}\boldsymbol{d}+\mu &=& 0 \quad \Big| \quad \cdot\big(\det\big[\boldsymbol{D}-\gamma\boldsymbol{J}\big]\big)^2 \\ \Longrightarrow \qquad \chi_4(\gamma) := \xi_4\gamma^4+\xi_3\gamma^3+\xi_2\gamma^2+\xi_1\gamma+\xi_0 &=& 0 \end{array}\right\} \tag{66}$$

with coefficients

$$\left.\begin{array}{rcl} \xi_4 &:=& \mu \\ \xi_3 &:=& 4\,(m_1\,d_2-m_2\,d_1) \\ \xi_2 &:=& 4\,m_{22}\,d_1^2-8\,m_{12}\,d_1\,d_2+4\,m_2\,d_1\,d_{12}-4\,m_1\,d_{22}\,d_1+4\,m_{11}\,d_2^2+4\,m_1\,d_2\,d_{12}-4\,m_2\,d_{11}\,d_2 \\ && -2\,\mu\,d_{12}^2+2\,\mu\,d_{11}\,d_{22} \\ \xi_1 &:=& 4\,m_2\,d_1\,d_{12}^2-4\,m_1\,d_2\,d_{12}^2+8\,m_{11}\,d_2^2\,d_{12}-8\,m_{12}\,d_2^2\,d_{11}+8\,m_{12}\,d_1^2\,d_{22}-8\,m_{22}\,d_1^2\,d_{12} \\ && +4\,m_1\,d_2\,d_{11}\,d_{22}-4\,m_2\,d_1\,d_{11}\,d_{22}-8\,m_{11}\,d_1\,d_2\,d_{22}+8\,m_{22}\,d_1\,d_2\,d_{11} \\ \xi_0 &:=& 4\,m_{22}\,d_1^2\,d_{12}^2-8\,m_{12}\,d_1^2\,d_{12}\,d_{22}+4\,m_{11}\,d_1^2\,d_{22}^2-8\,m_{22}\,d_1\,d_2\,d_{11}\,d_{12}+8\,m_{12}\,d_1\,d_2\,d_{11}\,d_{22} \\ && +8\,m_{12}\,d_1\,d_2\,d_{12}^2-8\,m_{11}\,d_1\,d_2\,d_{12}\,d_{22}+4\,m_2\,d_1\,d_{11}\,d_{12}\,d_{22}-4\,m_1\,d_1\,d_{11}\,d_{22}^2-4\,m_2\,d_1\,d_{12}^3 \\ && +4\,m_1\,d_1\,d_{12}^2\,d_{22}+4\,m_{22}\,d_2^2\,d_{11}^2-8\,m_{12}\,d_2^2\,d_{11}\,d_{12}+4\,m_{11}\,d_2^2\,d_{12}^2-4\,m_2\,d_2\,d_{11}^2\,d_{22} \\ && +4\,m_2\,d_2\,d_{11}\,d_{12}^2+4\,m_1\,d_2\,d_{11}\,d_{12}\,d_{22}-4\,m_1\,d_2\,d_{12}^3+\mu\,d_{11}^2\,d_{22}^2-2\,\mu\,d_{11}\,d_{12}^2\,d_{22}+\mu\,d_{12}^4. \end{array}\right\} \tag{67}$$

The *real* root $\gamma^\star$ of the four roots $\gamma_1^\star$, $\gamma_2^\star$, $\gamma_3^\star$, $\gamma_4^\star$ of the fourth-order polynomial $\chi_4(\gamma)$ as in (66) gives the desired intersection point in the quadrant of interest, i.e.,

$$\text{for cases (i) and (ii):} \quad \boxed{\boldsymbol{x}^\star(\gamma^\star)=-2\big[\boldsymbol{D}-\gamma^\star\boldsymbol{J}\big]^{-1}\boldsymbol{d}} \quad \text{and for case (iii):} \quad \boxed{\boldsymbol{x}^\star(\gamma^\star)=-2\big[\boldsymbol{D}-\gamma^\star\boldsymbol{J}\big]^{-1}\boldsymbol{d}+\boldsymbol{x}_\mathrm{s}}. \tag{68}$$

Note that there exist one, two, three or four real roots $\gamma_1^\star$, $\gamma_2^\star$, $\gamma_3^\star$, $\gamma_4^\star$ if the quadrics $Q_A(\boldsymbol{x})$ and $Q_B(\boldsymbol{x})$ do intersect; if the quadrics do not intersect there is no real root.

REFERENCES

[1] R. Teodorescu, M. Liserre, and P. Rodríguez, *Grid Converters for Photovoltaic and Wind Power Systems*. Chichester, United Kingdom: John Wiley & Sons, Ltd., 2011.

[2] C. Dirscherl, C. Hackl, and K. Schechner, "Modellierung und Regelung von modernen Windkraftanlagen: Eine Einführung," in *Elektrische Antriebe – Regelung von Antriebssystemen* (D. Schröder, ed.), ch. 24, pp. 1540–1614, Springer-Verlag, 2015.

[3] A. de Almeida, F. Ferreira, and J. Fong, "Standards for Efficiency of Electric Motors," *Industry Application Magazine*, vol. 17, pp. 12–19, Jan. 2011.

[4] Y. Wang, D. M. Ionel, M. Jiang, and S. J. Stretz, "Establishing the relative merits of Synchronous Reluctance and PM-Assisted Technology through Systematic Design Optimization," *IEEE Transactions on Industry Applications*, vol. 52, pp. 2971–2978, Jul. 2016.

[5] I. Boldea, L. N. Tutelea, L. Parsa, and D. Dorrell, "Automotive Electric Propulsion Systems with reduced or no Permanent Magnets: An Overview," *IEEE Transactions on Industrial Electronics*, vol. 61, pp. 5696–5711, Oct. 2014.

[6] E. Schmidt, "Synchronous reluctance machines with high-anisotropy rotors – comparison of their operational characteristics," in *Proceedings of the Australasian Universities Power Engineering Conference*, pp. 1–6, 2014.

[7] P. Zhang, D. Ionel, and N. Demerdash, "Saliency Ratio and Power Factor of IPM Motors with Distributed Windings Optimally Designed for High Efficiency and Low Cost Applications," *IEEE Transactions on Industry Applications*, vol. PP, no. 99, pp. 1–1, 2016.

[8] S. Vaez, V. I. John, and M. A. Rahman, "Adaptive Loss Minimization Control of Inverter-fed IPM Motor Drives," in *Proc. IEEE Power Electronics Specialists Conference (PESC)*, vol. 2, pp. 861–868 vol.2, Jun. 1997.

[9] R. S. Colby and D. W. Novotny, "An Efficiency-Optimizing Permanent-Magnet Synchronous Motor Drive," *IEEE Transactions on Industry Applications*, vol. 24, pp. 462–469, May 1988.

[10] N. Bedetti, S. Calligaro, and R. Petrella, "Stand-Still Self-Identification of Flux Characteristics for Synchronous Reluctance Machines Using Novel Saturation Approximating Function and Multiple Linear Regression," *IEEE Transactions on Industry Applications*, vol. 52, pp. 3083–3092, Jul. 2016.

[11] C. M. Hackl, M. J. Kamper, J. Kullick, and J. Mitchell, "Current control of reluctance synchronous machines with online adjustment of the controller parameters," in *Proceedings of the 2016 IEEE International Symposium on Industrial Electronics (ISIE 2016)*, (Santa Clara, CA, USA), pp. 153–160, 2016.

[12] C. Cavallaro, A. Di Tommaso, R. Miceli, A. Raciti, G. Galluzzo, and M. Trapanese, "Efficiency Enhancement of Permanent-Magnet Synchronous Motor Drives by Online Loss Minimization Approaches," *IEEE Transactions on Industrial Electronics*, vol. 52, pp. 1153–1160, Aug. 2005.

[13] R. C. Panaitescu and I. Topa, "Optimal Control Method For PMSM By Minimization Of Electrical Losses," in *Proc. IEEE International Conference on Optimization of Electrical and Electronic Equipments (OPTIM)*, vol. 2, pp. 451–456, May 1998.

[14] N. Urasaki, T. Senjyu, and K. Uezato, "A Novel Calculation method for Iron Loss Resistance suitable in modeling Permanent-Magnet Synchronous Motors," *IEEE Transactions on Energy Conversion*, vol. 18, pp. 41–47, Mar. 2003.

[15] R. Ni, D. Xu, G. Wang, L. Ding, G. Zhang, and L. Qu, "Maximum Efficiency Per Ampere Control of Permanent-Magnet Synchronous Machines," *IEEE Transactions on Industry Applications*, vol. 62, pp. 2135–2143, Apr. 2015.

[16] S. Y. Jung, J. Hong, and K. Nam, "Current Minimizing Torque Control of the IPMSM using Ferrari's Method," *IEEE Transactions on Power Electronics*, pp. 5603–5617, Dec. 2013.

[17] M. Preindl and S. Bolognani, "Optimal State Reference Computation With Constrained MTPA Criterion for PM Motor Drives," *IEEE Transactions on Power Electronics*, vol. 30, pp. 4524–4535, Aug. 2015.

[18] D. Schröder, *Elektrische Antriebe – Regelung von Antriebssystemen*. Springer, 2009.

[19] T. Gemassmer, *Effiziente und dynamische Drehmomenteinprägung in hoch ausgenutzten Synchronmaschinen mit eingebetteten Magneten*. PhD thesis, Elektrotechnisches Institut, KIT Karlsruhe, 2015.

[20] T. Finken, *Fahrzyklusgerechte Auslegung von permanenterregten Synchronmaschinen für Hybrid- und Elektrofahrzeuge*. PhD thesis, Insitut für elektrische Maschinen, RWTH Aachen, 2012.

[21] B. Cheng and T. R. Tesch, "Torque Feedforward Control Technique for Permanent-Magnet Synchronous Motors," *IEEE Transactions on Industrial Electronics*, vol. 57, pp. 969–974, Mar. 2010.

[22] S. Morimoto, Y. Takeda, T. Hirasa, and K. Taniguchi, "Expansion of operating limits for permanent magnet motor by current vector control considering inverter capacity," *IEEE Transactions on Industry Applications*, vol. 26, pp. 866–871, Sep. 1990.

[23] P. Niazi, H. A. Toliyat, and A. Goodarzi, "Robust Maximum Torque per Ampere (MTPA) Control of PM-Assisted SynRM for Traction Applications," *IEEE Transactions on Vehicular Technology*, vol. 56, pp. 1538–1545, Jul. 2007.
[24] J. Lemmens, P. Vanassche, and J. Driesen, "PMSM Drive Current and Voltage Limiting as a constraint Optimal Control Problem," *IEEE Journal of Emerging and Selected Topics in Power Electronics*, vol. 3, pp. 326–338, Jun. 2015.
[25] G. Schoonhoven and M. N. Uddin, "MTPA- and FW-Based Robust Nonlinear Speed Control of IPMSM Drive Using Lyapunov Stability Criterion," *IEEE Transactions on Industry Applications*, vol. 52, pp. 4365–4374, Sep. 2016.
[26] J. Kim, I. Jeong, K. Nam, J. Yang, and T. Hwang, "Sensorless Control of PMSM in a High-Speed Region considering Iron Loss," *IEEE Transactions on Industrial Electronics*, vol. 62, pp. 6151–6159, Oct. 2015.
[27] M. Preindl and S. Bolognani, "Model Predictive Direct Torque Control With Finite Control Set for PMSM Drive Systems, Part 2: Field Weakening Operation," *IEEE Transactions on Industrial Informatics*, vol. 9, pp. 648–657, May 2013.
[28] J. Ahn, S. b. Lim, K. c. Kim, J. Lee, J. h. Choi, S. Kim, and J. p. Hong, "Field Weakening Control of Synchronous Reluctance Motor for Electric Power Steering," *IET Electric Power Applications*, vol. 1, pp. 565–570, Jul. 2007.
[29] M. Tursini, E. Chiricozzi, and R. Petrella, "Feedforward Flux-Weakening Control of Surface-Mounted Permanent-Magnet Synchronous Motors accounting for Resistive Voltage Drop," *IEEE Transactions on Industrial Electronics*, vol. 57, pp. 440–448, Jan. 2010.
[30] L. Horlbeck and C. Hackl, "Analytical solution for the MTPV hyperbola including the stator resistance," in *Proceedings of the IEEE International Conference on Industrial Technology (ICIT 2016)*, (Taipei, Taiwan), pp. 1060–1067, 2016.
[31] K. Ueda, S. Morimoto, Y. Inoue, and M. Sanada, "A Novel Control Method in Flux-Weakening Region for Efficient Operation of Interior Permanent Magnet Synchronous Motor," in *Proc. IEEE International Power Electronics Conference (IPEC-ECCE ASIA)*, pp. 312–317, May 2014.
[32] C. M. Hackl, "Current PI-funnel control with anti-windup for synchronous machines," in *Proceedings of the 54th IEEE Conference on Decision and Control (CDC)*, (Osaka, Japan), pp. 1997–2004, 2015.
[33] C. M. Hackl, M. J. Kamper, J. Kullick, and J. Mitchell, "Nonlinear PI current control of reluctance synchronous machines," *arXiv:1512.09301 (see https://arxiv.org/pdf/1512.09301)*, 2015.
[34] D. Schröder, *Elektrische Antriebe - Regelung von Antriebssystemen (3., bearb. Auflage)*. Berlin: Springer-Verlag, 2009.
[35] M. Preindl and S. Bolognani, "Model Predictive Direct Torque Control With Finite Control Set for PMSM Drive Systems, Part 1: Maximum Torque Per Ampere Operation," *IEEE Transactions on Industrial Informatics*, vol. 9, pp. 1912–1921, Nov. 2013.
[36] C. Calleja, A. L. de Heredia, H. Gaztañ¿$\frac{1}{2}$aga, L. Aldasoro, and T. Nieva, "Validation of a Modified Direct-Self-Control Strategy for PMSM in Railway-Traction Applications," *IEEE Transactions on Industrial Electronics*, vol. 63, pp. 5143–5155, Aug. 2016.
[37] Z. Tang, X. Li, S. Dusmez, and B. Akin, "A New V/f-Based Sensorless MTPA Control for IPMSM Drives," *IEEE Transactions on Power Electronics*, vol. 31, pp. 4400–4415, Jun. 2016.
[38] G. Foo and X. N. Zhang, "Robust Direct Torque Control of Synchronous Reluctance Motor Drives in the Field Weakening Region," *IEEE Transactions on Power Electronics*, vol. PP, no. 99, pp. 1–1, 2016.
[39] T. Huber, W. Peters, and J. Böcker, "Voltage controller for flux weakening operation of interior permanent magnet synchronous motor in automotive traction applications," in *Proceedings of the IEEE International Electric Machines and Drives Conference*, pp. 1078–1083, 2015.
[40] W. Peters, O. Wallscheid, and J. Böcker, "Optimum efficiency control of interior permanent magnet synchronous motors in drive trains of electric and hybrid vehicles," in *Proceedings of the 17th European Conference on Power Electronics and Applications (EPE'15 ECCE-Europe)*, pp. 1–10, 2015.
[41] E. Rees, "Graphical discussion of the roots of a quartic equation," *The American Mathematical Monthly*, vol. 29, no. 2, pp. 51–55, 1922.
[42] H. Eldeeb, C. M. Hackl, and J. Kullick, "Efficient operation of anisotropic synchronous machines for wind energy systems," in *Proceedings of the 6th edition of the conference "The Science of Making Torque from Wind" (TORQUE 2016)*, Open access Journal of Physics: Conference Series 753, (Munich, Germany), 2016.
[43] S. Boyd and L. Vandenberghe, *Convex Optimization*. Cambridge University Press, (seventh printing with corrections 2009) ed., 2004.
[44] D. S. Bernstein, *Matrix Mathematics — Theory, Facts, and Formulas with Application to Linear System Theory*. Princeton and Oxford: Princeton University Press, 2nd ed., 2009.
[45] R. Nickalls, "The quartic equation: Invariants and Euler's solution revealed," *Mathematical Gazette*, vol. 93, no. 526, pp. 66–75, 2009.
[46] M. Abramowitz, I. Stegun, and D. Miller, *Handbook of Mathematical Functions With Formulas, Graphs and Mathematical Tables*, vol. (December 1972) of *Applied Mathematics Series*. Washington: National Bureau of Standards, 10^{th} ed., 1964.